Comptes Rendus

Géoscience

Sciences de la Planète

Marion Baques, Louis De Barros, Clara Duverger, Hervé Jomard, Maxime Godano, Françoise Courboulex and Christophe Larroque

Seismic activity in the Ubaye Region (French Alps): a specific behaviour highlighted by mainshocks and swarm sequences

Seismicity in France / *Sismicité en France*

Seismic activity in the Ubaye Region (French Alps): a specific behaviour highlighted by mainshocks and swarm sequences

Marion Baques[⊕] [*, *a*], **Louis De Barros**[⊕] [*a*], **Clara Duverger**[⊕] [*b*], **Hervé Jomard**[⊕] [*c*], **Maxime Godano**[⊕] [*a*], **Françoise Courboulex**[⊕] [*a*] **and Christophe Larroque**[⊕] [*a*]

[*a*] Université Côte d'Azur, CNRS, Observatoire de la Côte d'Azur, IRD, Géoazur, 250 rue Albert Einstein, Sophia Antipolis 06560 Valbonne, France

[*b*] CEA, DAM, DIF, F-91297 Arpajon, France

[*c*] Bureau d'évaluation des risques sismiques pour la sûreté des installations, Institut de Radioprotection et Sûreté Nucléaire, Fontenay-aux-Roses, France

Current address: CNRS-GEOAZUR – Campus Azur, 250, rue Albert Einstein, CS 10269, 06905, SOPHIA ANTIPOLIS Cedex, France (M. Baques)

E-mails: marion.baques@geoazur.unice.fr (M. Baques), louis.debarros@geoazur.unice.fr (L. De Barros), clara.duverger@cea.fr (C. Duverger), herve.jomard@irsn.fr (H. Jomard), maxime.godano@geoazur.unice.fr (M. Godano), francoise.courboulex@geoazur.unice.fr (F. Courboulex), christophe.larroque@geoazur.unice.fr (C. Larroque)

Abstract. The Ubaye Region is the most seismically active region in the Western Alps, with earthquakes that were commonly felt by the population and that even damaged local villages and cities. Since the first testimonies in 1844, this area has been regularly struck by seismic swarms with a high number of events, such as in 2003–2004 or 2012–2015, or by mainshock–aftershock sequences with a magnitude up to ML 5.3 in 1959. In this paper, we analysed both historical records and instrumental seismicity in the light of geological observations. Some earthquakes could be associated with known faults, even if most of them occurred on blind, unknown faults that reveal a highly fractured basement. The abnormal level of seismicity, together with its peculiar behaviour, suggests complex driving processes involving not only tectonic loading but also fluid pressure.

Keywords. Earthquake swarms, Fluid-driven process, Ubaye region, French Western Alps, Mainshock-aftershocks sequences.

Available online 8th September 2021

1. Introduction

Earthquakes usually occur as mainshock–aftershock sequences, which are interpreted as the release of the tectonic stress that build-up during the interseismic period. On the contrary, seismic swarms are characterized by a series of earthquakes clustered in time and space, with no clear mainshock [Hill, 1977, Scholz, 2002]. They can last for days to months [e.g., Bachura et al., 2021, Cheloni et al., 2017, D'Auria

---

et al., 2019, Ebel, 2016, Hauksson et al., 2019], which requires a forcing mechanism in order to maintain the activity. Earthquake swarms are common in volcanic regions such as Japan [Kodaira et al., 2002, Yukutake et al., 2011], Hawaii [Karpin and Thurber, 1987], Yellowstone [Farrell et al., 2009, 2010, Shelly et al., 2013a], as they are associated with magma upwelling or phreatic processes [McNutt and Roman, 2015]. They are also induced by anthropogenic activities in reservoirs, such as shale gas extraction or geothermal activities. For example, the massive storage of waste water produced by shale gas extraction in the Oklahoma state (US) induced a ~800-fold increase in the seismicity in 2016 compared to the pre-injection rate [Keranen et al., 2014, Schoenball and Ellsworth, 2017]. Swarms are also located in active tectonic zones with high deformation rate, like the Salton Trough swarm near the San Andreas Fault [Chen et al., 2012, Lohman and McGuire, 2007] or the Corinth rift [De Barros et al., 2020, Duverger et al., 2018]. In both volcanic and reservoir case and for some tectonic swarms, fluid perturbations can be easily evidenced [Chen et al., 2012, Duverger et al., 2015, Hainzl et al., 2016, Lohman and McGuire, 2007, Parotidis et al., 2003, Ruhl et al., 2016, Shelly et al., 2013b]. Earthquake swarms could also be found in subduction zones as in the Central Ecuadorian subduction zone [e.g., Segovia et al., 2018]. Such swarms, as well as some swarms in other tectonic settings, are associated with surface deformation, which reveals that they are triggered by slow, aseismic slips [Lohman and McGuire, 2007, Nishikawa and Ide, 2017, Rubin et al., 1999, Waldhauser et al., 2004]. Recent studies on swarms show that fluid diffusion and aseismic motion may be intertwined driving mechanisms [De Barros et al., 2020, Duverger et al., 2018, Eyre et al., 2020, Hatch et al., 2020]. Seismic swarms also occur in intraplate region with low deformation rate [Špičák, 2000] such as Arkansas [US, Chiu et al., 1984], Vosges [France, Audin et al., 2002], England, or Scotland [Assumpção, 1981] without evidence of either fluid or tectonic loading. For most of the tectonic swarms, the lack of direct observations on deformations and fluid processes at depth does not allow an easy and unambiguous interpretation of the driving mechanisms [e.g., Ruhl et al., 2016].

The Western Alps, between France and Italy, show low-to-moderate seismic activities with the presence of seismic swarms [Eva et al., 2020, Larroque et al., 2021]. Recently, swarms were observed in at least five main areas: Blausasc [10 km to Nice and Monaco; Courboulex et al., 2007], Vallorcine [between Chamonix, France, and Martigny, Switzerland; Fréchet et al., 2011], Maurienne Valley [50 km east of Grenoble; Guéguen et al., 2021], Sampeyre [80 km southwest to Turin, Italy; Godano et al., 2013], and the Ubaye Region, composed by the Ubaye and High Durance Valley [100 km to Nice and Grenoble; e.g., De Barros et al., 2019]. They can last for months (Blausasc, Vallorcine, Sampeyre) to years (Maurienne Valley, Ubaye Region). They are characterized by a large number of events, with more than 300 earthquakes recorded for each swarm, a low-to-moderate maximal local magnitude (between 3 and 4.8) leading to a maximal intensity (EMS-98) from III (Sampeyre) to V (other swarms). Therefore, some of them were felt by the population and caused slight damages in Vallorcine and the Ubaye area.

The most seismically active area in the Western Alps is the Ubaye Region, which mainly comprises the Ubaye Valley and the Durance Valley, close to the city of Barcelonnette (Figure 1). This 60 km long area is surrounded by the Chambeyron massif at the French–Italian border to the east, by the Serreponçon lake and the High Durance Valley to the west, and by the Argentera (Mercantour National Park) and Pelvoux (Ecrins National Park) massifs to the south and north, respectively. This area was not only struck by many swarm sequences [1977–1978, Fréchet and Pavoni, 1979; 1989, Guyoton et al., 1990; 2003–2004, e.g., Jenatton et al., 2007], but also by mainshock–aftershock sequences as in 1959 [Rothé and Dechevoy, 1967], 2012 [Thouvenot et al., 2016] and 2014 [De Barros et al., 2019] with local magnitude up to 5.3 in 1959 [Nicolas et al., 1998]. These moderate earthquakes were felt by the population and caused some damages to the buildings [Rothé and Dechevoy, 1967, Sira et al., 2012, 2014]. The seismic hazard is therefore a source of concern for the population.

The dual behaviour of the Ubaye Region is therefore peculiar, as a recurrent seismic activity occurred, with alternating mainshock–aftershocks sequences and swarms, even if the deformation rate in this area is very low [Masson et al., 2019, Walpersdorf et al., 2018]. It raises the question of the processes at depth that can trigger and drive such seismic behaviours. Therefore, studies on this region highlighted the need of complex processes that involve tectonic loading
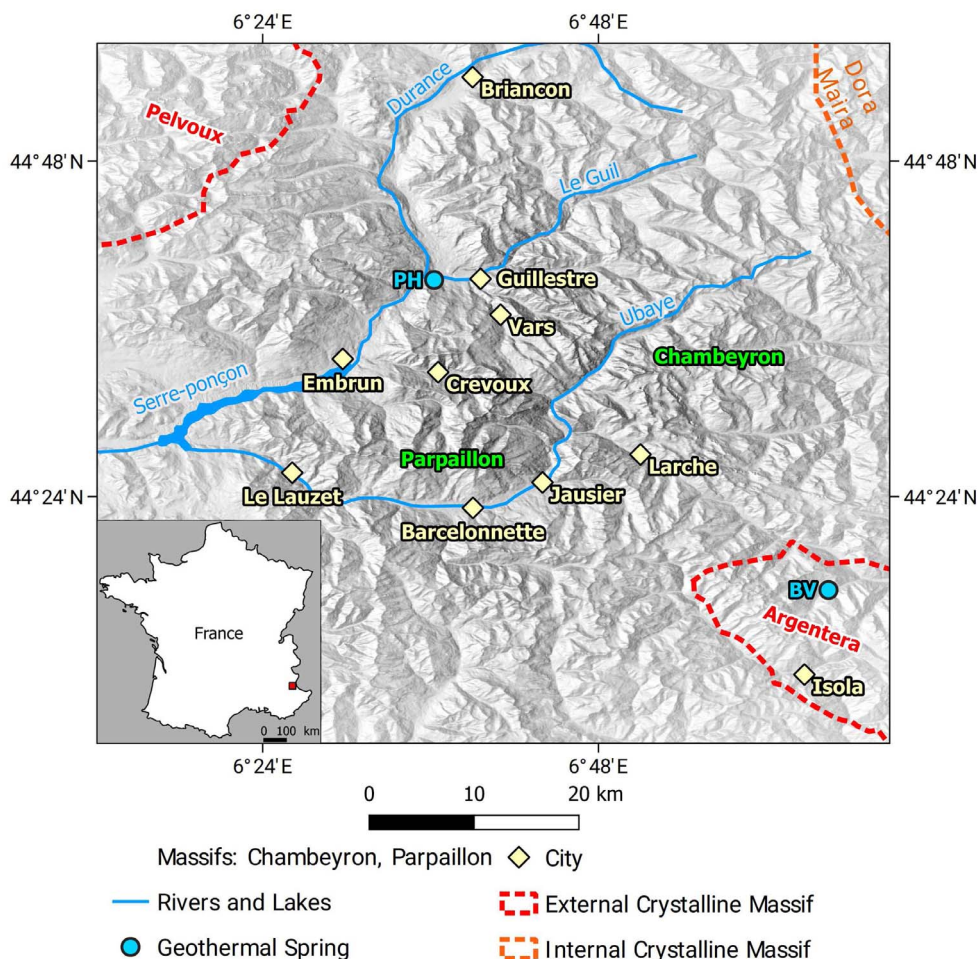
Figure 1. Topographic map of the Ubaye Region, with the main cities, rivers, massifs, and geothermal springs (BV: Bagni di Vinadio, PH: Plan de Phazy).

and fluid overpressure [Daniel et al., 2011, De Barros et al., 2019, Jenatton et al., 2007, Leclère et al., 2012, 2013, Thouvenot et al., 2016]. To explore this complex behaviour, we here propose a review on the existing studies about this area. We first present the geological context of the Ubaye Region, before showing the seismic activity from 1590 to the present day. We then discuss the specificity of the seismic behaviour in order to explore the potential processes that drive this activity.

2. Geological context

The Alpine belt results from the collision between the continental margins of the African and European plates following their convergence and the subduction of the Tethys ocean during the Cenozoic [Handy et al., 2010, Stampfli et al., 2002, Tricart, 1984]. The main structures of the Western Alps are distributed in the internal zone in the east and the external zone in the west, which are separated by the Frontal Penninic Thrust [Ricou and Siddans, 1986; Figure 2]. The Ubaye River is a main stream of the southwestern Alps. Its valley crosses the Frontal Penninic Thrust, as it first flows in the Briançonnais unit, belonging to the internal zone, and then in the Dauphinois unit, which belongs to the external zone (Figure 2). The Briançonnais unit is composed of a pile of thick metamorphic nappes [Sue et al., 2007b]. The Dauphinois unit is composed of 1 to 2 km thick Mesozoic
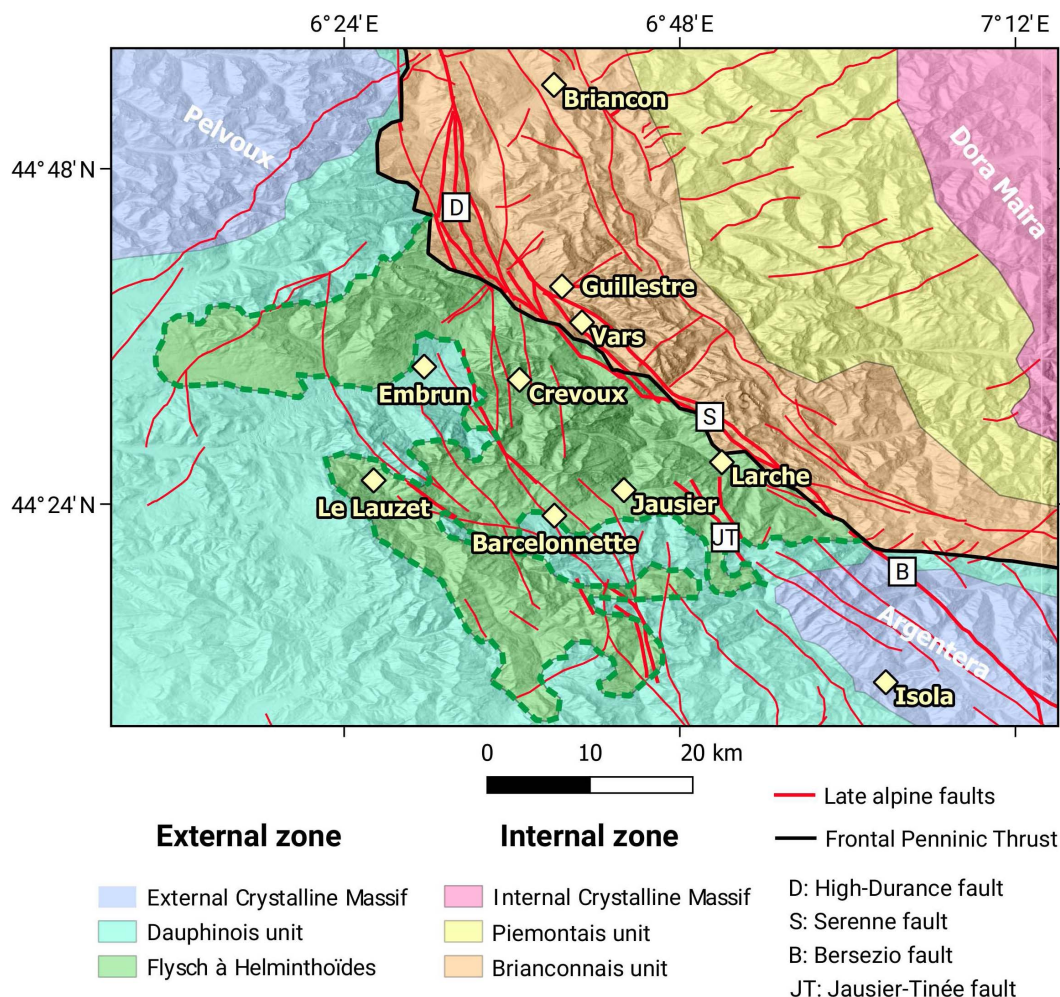
Figure 2. Structural scheme of the Ubaye Region showing the main geological units and the main fault traces. The black line corresponds to the Frontal Penninic Thrust and the red lines to the trace of the late alpine faults from Tricart [2004]. The major faults have wider red lines.

to Cenozoic sedimentary rocks [sandstone, marls, and limestone, Kerckhove et al., 1978; Figure 2] that forms the sedimentary cover of the external crystalline massifs represented north and south of the Ubaye Valley by the Pelvoux and Argentera massifs, respectively (Figure 2). Above the Dauphinois unit, the "Flysch à Helminthoïdes" thrust sheet [also called "Embrunais–Ubaye nappes" by Kerckhove, 1969] is composed by late Cretaceous turbiditic series that were thrusted westward during the Oligocene period [Fry, 1989, Gratier et al., 1989].

As a consequence of the long-lasting geological history of the Western Alps, the geological formations are highly deformed and fractured. In the following,

we mainly focus on the description of the faults considered as late alpine faults [Kerckhove, 1969, Tricart, 2004]. They correspond to the ones that were reactivated during the last setting of the chain, that show nowadays indices of neotectonic activities [Sue, 1998, Sue et al., 2007b] and along which the seismic activity currently seems to develop [Jenatton et al., 2007, Le Goff et al., 2009, Mathey et al., 2020, Sanchez et al., 2010, Sue et al., 2007b].

In the crystalline basement of the Argentera massif, the major faults are mainly NW–SE with dip close to the vertical. Several faults can be seen connecting to each other over a width of about 20 km. This system of faults continues towards the northwest

under the Ubaye–Embrunais area even if we cannot describe it in detail [Kerckhove, 1969, Sue and Tricart, 2003, Tricart and Schwartz, 2006]. The major faults present in the Ubaye Region are the High Durance fault, the Serenne fault, and the Bersezio fault (Figure 2). The Serenne fault is the surface tip of the Frontal Penninic Thrust, whilst the High Durance and the Bersezio faults are the prolongations towards the northwest and the southeast, respectively, of the Serenne fault (Figure 2). The Jausier–Tinée fault is a fault system parallel to and at about 20 km south of the Serenne fault. These faults are partly hidden below the sedimentary units, but they might be extended in the Argentera massif, where they are outcropping. Therefore, the observations of these outcropping faults may help characterize the hidden fault system at depth below the Ubaye–Embrunais area.

Some of the recent seismicity occurred on or close to these faults, showing that these faults are still active. At least three historical earthquakes could be associated to the High Durance fault (27th November 1884, 12th July 1904, 19th March 1935), with a still persistent activity on this fault area [Mathey et al., 2020, Sue et al., 1999]. Recent seismic activity in the Ubaye Region was also observed close to the Serenne fault [Sue et al., 2007a] or to the Jausier–Tinée fault [Jenatton et al., 2007]. However, most of this seismicity cannot be unambiguously related to known fault traces. The Flysch of the Embrunais–Ubaye Nappes are indeed too compliant to preserve the fault trace if the rupture reaches the surface. It is therefore difficult to find and see the outcropping traces of the still active faults in this area. For example, the ML 4.8 and ML 5.1 earthquakes, occurring respectively in 2012 and 2014, took place on blind, unknown faults [Sira et al., 2012, 2014].

The seismic mechanisms in the Ubaye Region show a dominant extensional regime with a strike-slip component. Fojtíková and Vavryčuk [2018] gathered the published mechanisms for the 2003–2004 and 2012–2015 swarms and inverted them to infer the stress state. They obtained a $\sigma 1$-axis-oriented N29° E and plunging 61° SE; a $\sigma 2$-axis-oriented N188° E and plunging 27° SW; and a sub-horizontal $\sigma 3$-axis-oriented N283° E, with a stress ratio (R-ratio) of 0.38. The Ubaye Region is therefore characterized by a transtensional stress regime according to the orientation of the principal stress axes and the

R-ratio [Fojtíková and Vavryčuk, 2018]. Other stress state computations [Delacou et al., 2004, Eva and Solarino, 1998, Leclère et al., 2013] also reveal such extensional regimes with slight changes in the stress orientations.

The strain rate in this Ubaye Region was measured using satellite geodesy [Nguyen et al., 2016, Nocquet et al., 2016, Serpelloni et al., 2013, Walpersdorf et al., 2018]. It shows a small uplift of 0.5 mm/yr in the Ubaye Region without significant horizontal strain. Different processes can explain this uplift: counter-clockwise rotation of the Apulian plate [e.g., Serpelloni et al., 2007], isostatic adjustment in response of erosion process [e.g., Vernant et al., 2013], post-glacial rebound [e.g., Barletta et al., 2006], or post-slab-detachment rebound [e.g., Gardi et al., 2010]. Recent studies [e.g., Sternai et al., 2019] agreed that several processes are needed to explain the deformation occurring in the Western Alps and the present-day extensional regime in the Ubaye Region [e.g., Sue et al., 2007a,b].

3. Seismicity

According to the available records, the seismic activity can be split in two parts. While only testimonies and field markers can be used to reconstruct the seismic activity before 1965, the installation of national [LDG, RESIF, 1995] and local (Sismalp) seismic networks [Larroque et al., 2021] allows then finer analysis of the seismicity.

3.1. *Historical seismicity*

Before the installation of seismic networks, earthquakes are only known from the analysis of archives (local and/or regional newspapers, felt reports by the population, etc.) describing their impact on buildings and infrastructures as well as effects on the population and the environment. The knowledge we have about earthquakes while going back in time strongly depends not only on the strength of the events but also on local geographical and historical contexts. In this section, we used data contained within the SisFrance database [Jomard et al., 2021, Scotti et al., 2004] in order to discuss both the location and the behaviour of historical earthquakes in and around the Ubaye Region.
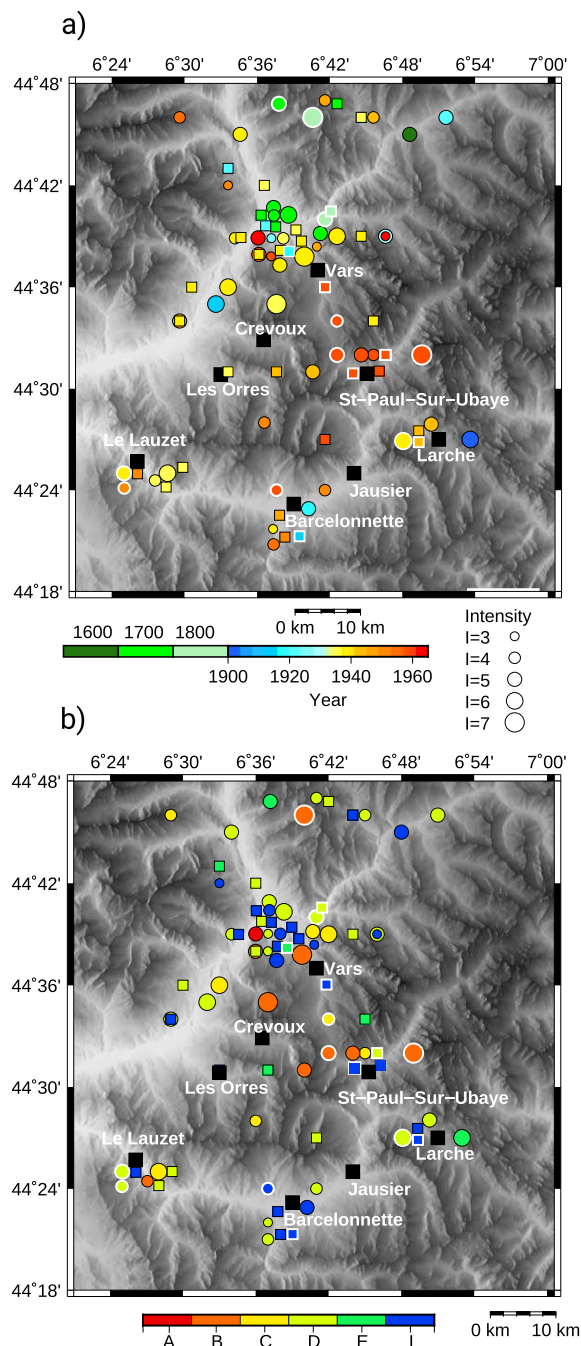
a)

b)

Figure 3. Location map of the historical seismicity. (a) Location of the historic earthquakes coloured by the occurring year from SisFrance database [Scotti et al., 2004]. (b) Location of historic earthquakes coloured by the location uncertainty, with: A: few km, B: ~10 km, C: ~20 km, D: ~50 km, E: arbitrarily defined, I: isolated.

Figure 3. (**cont**.) On both panels, circles show events scaled by estimated intensity, while the coloured squares are events with no determined intensity. The white border on symbols indicates the presence of several events at the same period. The black squares are the main cities. Near Le Lauzet, Barcelonnette, and northwest of Vars, the superimposed earthquakes have been artificially dispersed for better visualization.

The oldest event reported so far in SisFrance in the area dates back from 1590 (Guil Valley), and several other earthquakes were reported in 18th century in Durance Valley. These ancient testimonies could be mainly explained by the presence of important cities settled in the Durance Valley (e.g., Embrun), as well as historical strongholds (e.g., Mont-Dauphin located eastward of Guillestre and Briançon). On the other hand, the first event reported within the Ubaye Valley occurred in 1844, which is very recent and is probably due to the low population density in this area, but also to the rural character of the habitat and the economy within the valley at the time. As a consequence, the information we have on historical earthquakes, especially within the Ubaye Valley, is highly incomplete and results in strong uncertainties, being driven by the location of human settlements as well as the economic development of valleys.

To analyse the data contained in the SisFrance database, we first went back to the original documents (archives) with the aim to understand whether the reported earthquakes were followed or preceded by other events not individually listed in the database, and whether the number of events and their temporal organization are compatible with the occurrence of a swarm sequence (Figures 3, 4a). Secondly, we analysed the location of earthquakes in the light of their reported uncertainties in order to evaluate if these locations correlate with instrumentally recorded events and with the location of potentially active faults.

Epicentre locations of the earthquakes reported in the SisFrance database (from year 1590 to 1965) are plotted in Figure 3(a), whether or not the intensity of the epicentre has been determined. In Figure 3(b), we present the uncertainty related to the location of these events, following the quality scale [QPOS

parameter, Jomard et al., 2021, Scotti et al., 2004] determined in SisFrance from the quality and location of the individual testimonies reporting the events. The event location qualities from A to D indicate an increasing uncertainty from a few kilometres up to 50 km. The quality E indicates an arbitrary location when few poorly constrained data are present, while the quality I indicates an isolated location, which corresponds to the location of a single testimony. This last category could also indicate a low intensity event felt only locally. Similarly, the uncertainty related to the level of the epicentral intensity (MSK-64) increases from 1 to 3 (well constrained to poorly constrained), 4 and 5 indicating an arbitrary or isolated intensity, respectively (Figure 4a).

Among the 127 events reported before 1965, there were at least 23 events with an intensity equal to or greater than V (i.e., producing slight damages and frightening people). The maximal intensity reported in the catalogue is related to the 5th of April 1959 earthquake, with an intensity VII–VIII [MSK-64, Rothé and Dechevoy, 1967]. At first glance, there are more historical earthquakes reported in the Durance Valley than in the Ubaye Valley, which could be a bias due to the presence of cities and military strongholds in the north. This heterogeneity in the testimonies between the north and the south of this area could also affect the location of some events for which no or only few reports are available in the Ubaye Valley. Similarly, the apparent increase in the number of events with time is also likely to be related to an increase of testimonies rather than to an actual change in the seismic rate.

Figure 4(a) represents the temporal distribution of the historical seismicity, which is also summarized in Table 1. Most of the events were observed scattered in time and space, but several periods show clusters of seismic activity:

- The 1780–1785 cluster is composed of six events with a maximum intensity of VI (29th April 1785). This group of events is located at the confluence between the Durance and Guil rivers near Guillestre (Figure 3, Table 1), but their large location uncertainty makes their spatial clustering doubtful. For example, two events reported in Mont-Dauphin on the 12th of September 1785 are more likely linked to a stronger event that oc-
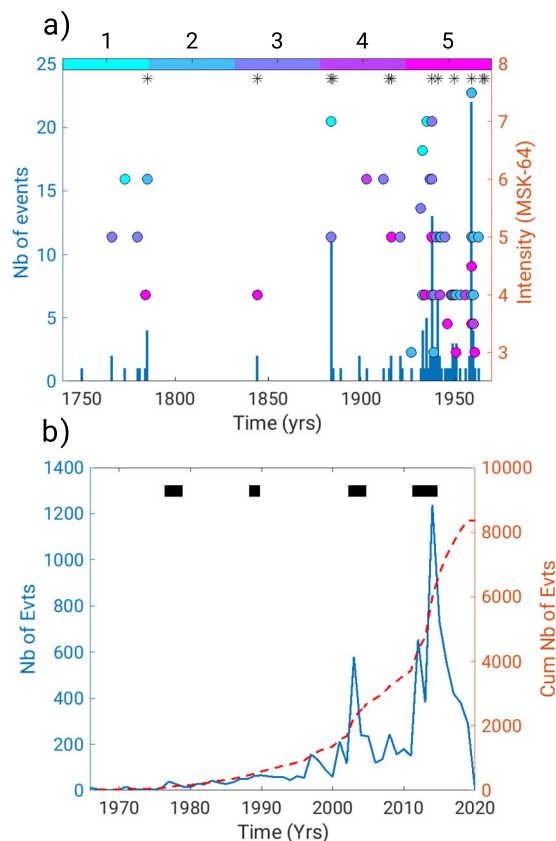

Figure 4. Temporal distribution of the seismicity. (a) Historical seismicity. The left axis corresponds to the number of events per year shown as bars, while the dots indicate the estimated intensity (right axis). The colour of the intensity corresponds to the intensity uncertainty with 1: sure, 2: pretty sure, 3: not sure, 4: arbitrarily, 5: isolated. The stars show the presence of several events at the same period. (b) Temporal distribution for the Instrumental seismicity. The blue line shows the number of events per year (left axis) while the red dashed line is the cumulated number of events (right axis). The black bar corresponds to the duration of the identified swarms.

curred few minutes before in the Sousa Valley more to the north with an epicentral intensity of VII.

- The 1884–1885 cluster corresponds to twelve events located near Guillestre and most probably some kilometres north of the city.

Table 1. Swarms and group of events in the Ubaye Region

Date	Number of earthquakes located/detected	Maximum magnitude (ML)	Maximum intensity	Depth (km)	Lieu	References
1780–1785	7 (d)	-	VI	-	Mont-Dauphin	Si
1844	2 (d)	-	IV	-	Barcelonnette	Si
1884–1885	12 (d)	-	VII	-	Guillestre	Si
1915	QQ (d)	-	-	-	Barcelonnette	Si
1916	QQ (d)	-	-	-	Guillestre	Si
1933	4 (d)	-	VII	-	Le Lauzet	Si
1935	5 (d)	-	VII	-	Durance-Guil confluence	Si
1937–1938	12 (d)	-	VII	-	Guillestre, Embrun	Si
1938	3 (d)	-	V	-	Le Lauzet	Si
1941	6 (d)	-	-	-	Larche	Si
1950	2 (d)	-	IV	-	Le Lauzet	Si
1959	23 (d)	5.9	VIII	8	St-Paul-sur-Ubaye	Ni, Si
1965–1966	5 (d)	-	IV	-	Barcelonnette	Si
1977–1978	200 (l)	3.6	-	0–13	Chambeyron	Fr
1989	250 (l)	3.4	-	10	Chambeyron	Gu
2003–2004	1616 (l)	2.7	-	3–8	Jausier	Je
2012–2016	6000 (l)	4.8	V–VI	4–11	Crevoux	Th, Db, Sir

Si: SisFrance database [Scotti et al., 2004], Ni: Nicolas et al. [1998], Fr: Fréchet and Pavoni [1979], Gu: Guyoton et al. [1990], Je: Jenatton et al. [2007], Th: Thouvenot et al. [2016], Db: De Barros et al. [2019], Sir: Sira et al. [2012, 2014], (d): detected events, (l): located events, QQ: more than one events felt.

The crisis started on the 23rd of November with the strongest event occurring on the 27th and had a maximal intensity of VII, with a good intensity and location uncertainty (1 and B, respectively). The last event occurred in early January.

- During 1915–1916, two distinct areas were struck by earthquakes with only some events reported. The first period started in December 1915, where some shakings were felt by the population in Barcelonnette and lasted until February 1916 when an earthquake of an epicentral intensity of V occurred, however not mentioned elsewhere. In September 1916, some earthquakes have been felt in Guillestre and in some villages in the Queyras Valley (northeast of Guillestre). The events are poorly known and it is not possible to exclude that they had a common source.
- The cluster in 1933 contains four events occurring within five days at the end of September with the strongest event at the start of the crisis. These events are located in the Le Lauzet area with a maximal intensity of VI–VII (Figure 3, Table 1) and are associated with a small uncertainty of 1 and B for intensity and location, respectively.
- In 1935, one of the strongest earthquake known in the region occurred in an area between Crevoux and Vars. The crisis started on the 19th of March with an event of epicentral intensity Io = VII and was followed by four events with undetermined intensities during the next five days. The location uncertainty varies from the B to the I, with the best quality for the strongest event (Figure 3, Table 1).
- The seismicity in 1937–1938 is composed of more than ten reported events occurring nearby Guillestre city, with a maximal intensity of VII. The crisis started in December 1937 with two shocks of Io = VI and ended in September 1938 with the strongest event occurring in July (Io = VII). Considering the locations of all these events,

an epicentre area located somewhere between Guillestre, Vars, and Embrun may be favoured, close to the 1935 one. In addition to these events, a second cluster composed of three events with a maximal intensity of V is located in the Le Lauzet area (Figure 3, Table 1). The two sequences are more probably independent from each other, even if the location of the second one is uncertain.

- From February 1941 until March 1942, nine events were reported. It began on the 23rd of February 1941 by a foreshock, followed by an intensity Io = VI event and five aftershocks, most of them being reported in the area of Larche, near the Italian boundary. However, the mainshock has been reported in SisFrance as occurring in Italy near Prazzo. Considering both the hour and the macroseismic data reported in SisFrance, this earthquake occurred most probably near Larche as well. In October the same year, an earthquake occurred near Vars, felt both in Barcelonnette and St Clément near Guillestre city. On the 15th of March 1942, a stronger event (Io = V) occurred in the same area. These two sequences appear to be independent from each other.
- The sequence in 1959 contains 23 events (Figure 4a), and is located near St-Paul-sur-Ubaye (Figure 3, Table 1). This sequence started with one of the strongest events in the Western Alps (intensity of VII–VIII, MSK-64) on the 5th of April 1959 [ML = 5.3, Nicolas et al., 1998]. It was felt in Grenoble, Nice, and in Italy. Two children were injured and many damages were reported [collapsed walls, chimneys, and rock falls, etc.; Rothé and Dechevoy, 1967]. Between 5th April 1959 and 17th July 1959, 20 aftershocks were detected with a maximum intensity of V (SisFrance database), and were felt by the population. The activity continued until the 8th of May of the next year. There is discussion about the location of the 5th of April earthquake, because the instrumental data and testimonies lead to locations ~20 km away from each other. Using testimonies and an intensity map, the epicentre is found few kilometres east of St-Paul-sur-Ubaye [Rothé

and Dechevoy, 1967; Figure 3a,b] spatially correlated with the Serenne Fault. The instrumental location, more to the west, is obtained using data from 26 stations [Nicolas et al., 1998] and it is more compatible with the southern prolongation of the High Durance fault (Figure 5a). Looking at the spatial distribution of the aftershocks, especially those occurring on the 19th of April (Io = IV) and the 17th of April (Io = V), and considering that these aftershocks happened in the same area as the mainshock, one could consider that the epicentre area of the main event is more likely located near the Vars pass, i.e., compatible with the macroseismic field in SisFrance.

- Finally, the last pre-instrumental cluster of seismicity occurred in 1965–1966 and is composed of five events with a maximal intensity of IV (MSK-64), located nearby Barcelonnette (Figures 3, 4(a), Table 1), despite a strong location uncertainty (D). The crisis started in September 1965 and ended in early January 1966, with the strongest event occurring in early December 1965.

With the description of the historical temporal distribution, four independent seismic zones, with recurrent activities may be highlighted: a wider area encompassing Guillestre to the north and St-Paul-sur-Ubaye to the south (1780–1785?, 1884–1885, 1935, 1937–1938, 1942, 1959), Le Lauzet (1933, 1938, 1949–1950), Barcelonnette (1844, 1915?, 1965), and Larche (1903, 1941, 1943). However, as the location is poorly constrained, it is not possible to infer if the recurrent seismic activity occurred at same locations and on same faults, nor to associate it to known faults. Finally, except for the 1959 sequence, it is difficult to classify the clusters of seismicity as either swarms or (foreshock-) mainshock–aftershock sequences. Some sequences might look like mainshock–aftershock sequences as the 1933 and 1935 ones. Indeed, the strongest event occurred at the start of the crisis and the following events could be seen as aftershocks. The 1884–1885, 1937–1938, and 1965–1966 sequences might be interpreted as swarms, as the strongest event occurred in the middle of a long-lasting (several months) sequence. However, the events occurring before the strongest
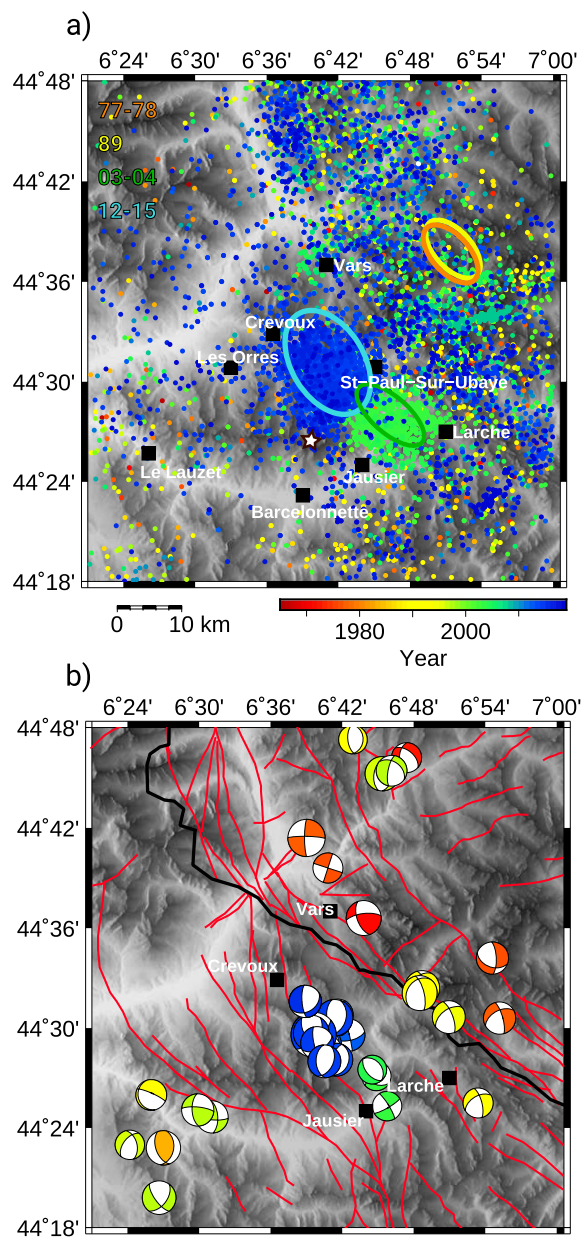
a)

b)

Figure 5. Location map of the instrumental seismicity. (a) Earthquake epicentres from 1965 to 2020 (LDG catalogue). The orange, yellow, green, and blue ellipses show the 1977–1978, 1989, 2003–2004, and 2012–2015 swarms, respectively. The star corresponds to the instrumental location of the 5th of April 1959. (b) Map of the focal mechanisms [Leclère et al., 2013, Mazzotti et al., 2021, Thouvenot et al., 2016] from 1965 to 2020 with a magnitude greater than 2.5.

Figure 5. (**cont**.) The size of the mechanisms associated with the magnitude and the colours to the year. The red lines corresponding to the late alpine faults, the black one, to the Frontal Peninnic Thrust, from Tricart [2004].

one might also be seen as foreshocks, or the cluster as a quick succession of several mainshock events.

In conclusion, the region has been regularly active since the oldest records dating from 1590. The earthquakes show a low-to-moderate intensity, and mostly occur on unknown faults, as swarms or mainshock sequences. It is worth noting that the widest area encompassing the city of Guillestre and the villages of St-Paul-sur-Ubaye, Vars, and Crevoux seems to be a privileged place of recurrent seismic activity, with the strongest events recorded regionally.

3.2. *Instrumental seismicity*

Instrumental data started in 1962 with the installation of the LDG network at the national scale [Duverger et al., 2021]. In 1981, the short period triggered stations that composed the Sismalp network (https://sismalp.osug.fr) were specifically installed to monitor the seismicity in the Alps. The first continuous station in the Ubaye area (SURF), belonging nowadays to the RESIF network (http://seismology.resif.fr), was settled in October 1989. Since 2006, SURF has been a continuous, broadband, three-component station. The LDG catalogue is the longest in time and the most homogeneous instrumental catalogue that we have in the Ubaye Region. Therefore, we use this catalogue to analyse the seismic activity after 1965 (Figure 5a).

From 1965 to nowadays, about ~13,000 earthquakes (Figure 4b) occurred, with local magnitudes below 5.2. The apparent increase of the activity with time, as seen in Figure 4(b), is directly linked to the improvement of the seismic network [Duverger et al., 2021]. Nearly half of them are associated with the swarms that occurred in 2003–2004 and 2012–2015 in the external zone between the localities of Crevoux and Jausier (Figures 4, 5a). In the Briançonnais unit to the north and east, the seismicity is less clustered in space and time and gathers in a wide corridor around the High Durance and Serenne faults. The 1977–1978 and 1989 swarms seem also located in

this area, within the internal zone, even if the depth uncertainties and their proximity with the inclined Frontal Penninic Thrust make it questionable. To the west and south of the Ubaye Region, the seismic activity is lower and scattered.

Since 1965, four swarm episodes have been unambiguously observed (Figure 4(b), Table 1). The small burst in 1977–1978 corresponds to a swarm sequence with magnitudes from ML −0.5 to ML 3.6 [Fréchet and Pavoni, 1979]. This swarm activity (Figure 5(a), Table 1) was recorded by two 1-month long temporary seismic networks of respectively 11 and 16 stations. During the first temporary deployment in September–October 1977, Fréchet and Pavoni [1979] detected 1500 events and located 150 events, with an epicentral uncertainty of 1 km. During the second one in September–October 1978, 50 events were located out of 300 detected events, with an epicentral location uncertainty of 500 m. This swarm extends from 0 to 13 km depth, which correspond to the sedimentary covers and the crystalline basement (absolute uncertainty greater than 1 km) beneath the Chambeyron massif. Most of the events are located in the crystalline basement and do not seem to align on a unique fault plane but scatter on a wide zone. Several focal mechanisms were computed that show either normal or right-lateral strike-slip motion on fault planes oriented N–S to N140° E [Fréchet and Pavoni, 1979; Figure 5b]. The epicentres are within the Briançonnais unit (internal zone). However, the uncertainties on the depth make difficult to determine if this swarm is located in the external or internal zone due to its promiscuity to the dipping Frontal Penninic Thrust.

A second swarm occurred from 22nd to 29th January 1989 [Guyoton et al., 1990; Figure 5(a), Table 1]. Guyoton et al. [1990] detected 250 events, seven of which have a magnitude between ML 2.4 and ML 3.4. The events were located (absolute hypocentre location uncertainty of 1 km) beneath the Chambeyron massif (10 km depth) at a similar location as the 1977–1978 swarm. They also computed two focal mechanisms that show right-lateral strike-slip motion, with orientation similar to the Serenne fault [Guyoton et al., 1990; Figure 5b].

In 2003–2004, an abnormally high seismic activity, as shown by the strong increase in the cumulated number of events, is caused by another swarm (Figure 6a,c). More than 16,000 earthquakes were recorded with magnitude ranging from ML −1.3 to ML 2.7. Among them, about 200 events with magnitude down to ML 1.3 were felt at La Condamine-Châtelard, a small town located just above the swarm, 5 km north of Jausier (Table 1). Figure 7(a) presents the temporal distribution of the 2003–2004 seismic activity for 974 events that were relocated through a double-difference algorithm [Daniel et al., 2011]. The seismic activity increased slowly from the beginning of 2003 until July 2003, and then remained at a high level for about 3 months. The maximal magnitude (ML = 2.7) event occurred in the middle of the seismic sequence. The seismic rate then slowly decayed to reach a background level towards the summer of 2004, despite some episodes of high activity in late 2004 and early 2005 (Figures 4b, 5a, 6c, 7a). The event locations describe a 9 km long alignment oriented ~N150° E [Jenatton et al., 2007; Figure 6c]. All seismic activity occurred between 3 and 8 km depth, within the crystalline basement. Jenatton et al. [2007] computed the focal mechanisms for 38 events, later extended to 74 events by Leclère et al. [2013]. The events show right-lateral strike-slip motions along N150 to N175° E structures with small extensional components as well as normal-slip motions with a small strike-slip component (Figure 5b). For both mechanisms, nodal plane orientations are similar to the main extensional direction of the cluster [~N150° E, Jenatton et al., 2007] and to the orientation of the Jausier and neighbouring faults.

Within the swarm, an apparent migration of the seismicity can be observed from the NW to the SE [Daniel et al., 2011, Jenatton et al., 2007, Leclère et al., 2013, 2012, Thouvenot et al., 2016]. Figure 8(a) represents the spatio-temporal distribution of the crisis in a distance versus time plot. The seismic front can be fitted by a hydraulic diffusion law [Shapiro et al., 2002], with a diffusivity of 0.005 m^2/s (Figure 8a), similar to the one found by Jenatton et al. [2007]. Such value is consistent with fluid diffusivity observed in other swarm sequences [e.g., Duverger et al., 2015]. Daniel et al. [2011] and Leclère et al. [2012, 2013] calculated the fluid overpressure needed to explain the migration. Daniel et al. [2011] fitted the seismicity rate recorded at one station using a stochastic epidemic-type aftershock sequence model. Then, using a rate-and-state framework, they converted the estimated background seismicity
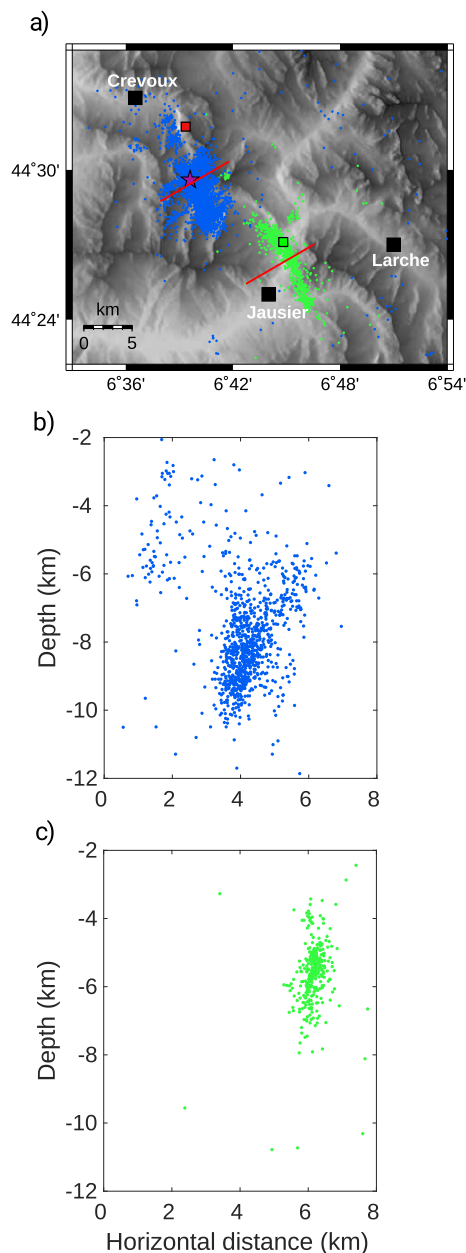
a)

b)

c)

Figure 6. Location map of the 2003–2004 swarm, in green from Daniel et al. [2011], and of the 2012–2015 (blue, Thouvenot et al. [2016]). The red lines show the positions of the cross-section represented in (b) and (c). (b) N60° E cross-section for the 2012–2015 swarm, and in (c) for the 2003–2004 swarm. For both cross-sections, only the seismicity within 1 km of the red lines in (a) is shown. In (a) the purple star corresponds to the 2012 and 2014 mainshocks.

Figure 6. (**cont**.) The position of this star also corresponds to the origin point for the spatio-temporal distribution represented in Figure 8. The green and red squares corresponding to the origin point for the 2003–2004 and the swarm-like spatio-temporal distribution, respectively.

rate to changes in effective stress and in fluid pressure. They found that a relative overpressure change of 8 MPa explained the change of the seismicity rate. After inverting focal mechanisms to reconstruct a local stress state, Leclère et al. [2013] used Cauchy's equations to estimate a fluid overpressure of 20-to-50 MPa. In conclusion, the 2003–2004 swarm is characterized by a rupture zone of 15 km^2 along a N145–175° E fault plane and a migration from NW to the SE. This swarm is likely to be driven by a fluid-pressure diffusion, with a hydraulic diffusivity of 0.005 m^2/s and an overpressure between 8 and 50 MPa.

The latest crisis started in 2012 and continued until 2019, with the largest period of activity between 2012 and the end of 2015 (Figure 4b) and a few smaller bursts of activity in 2016 and 2017. We later refer to this period as the 2012–2015 swarm, following Thouvenot et al. [2016]. It is located 10 km northwest of the 2003–2004 swarm (Figures 5a, 6a). The crisis started by a Mw = 4.3 (ML = 4.8) earthquake on 26th February 2012, and was followed two years later by a Mw = 4.8 (ML = 5.1) event, on 7th April 2014 (Figure 7b). Both events occurred approximately at the same location, except that the 2014 event is found deeper (9.9 km depth) than the 2012 one (8.8 km depth). No depth uncertainty was provided by Thouvenot et al. [2016], then the question about the significance of the depth difference between the two mainshocks could be raised. After both mainshocks, the seismicity decreased as an aftershock sequence (Figure 7b). This decay, fitted by a modified Utsu–Omori's law [Utsu, 1961], is however, slower than usual, with $p = 0.77$ for the 2014 aftershocks [De Barros et al., 2019]. After the 2014 event, other mainshock–aftershock sequences were observed in April and November 2015 with magnitudes of Mw = 3.4 and Mw = 4.2, respectively. The 2012–2015 sequence can be therefore seen as a quick succession of mainshock–aftershock sequences. However, the full
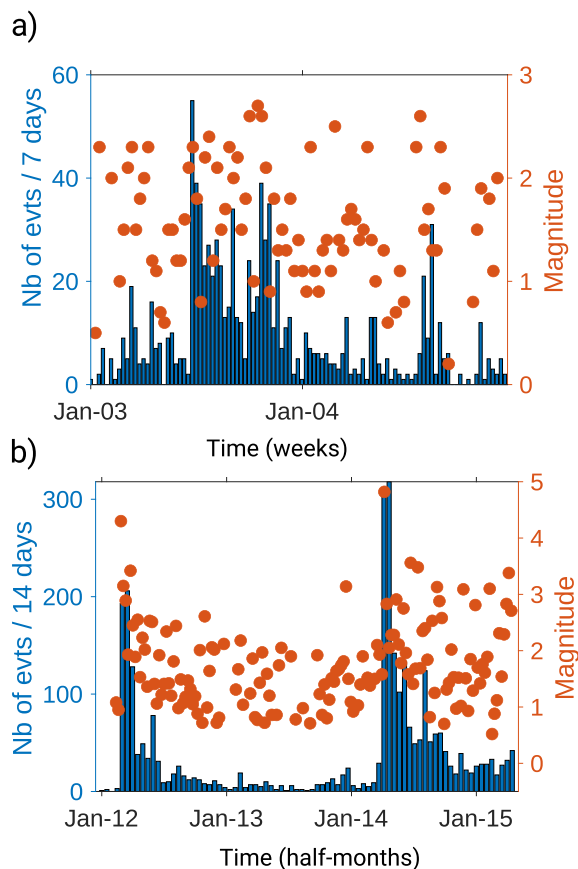
a)

b)

Figure 7. Temporal distribution of the seismicity during (a) The 2003–2004 and (b) The 2012–2015 swarms. (a) Weekly number of events (bars) and maximal magnitude (red dots) for the 2003–2004 swarm. The catalogue is from Daniel et al. [2011]. (b) Two-weeks number of events (bars) and maximal magnitude (red dots) for the 2012–2015 swarm. Catalogue is from Thouvenot et al. [2016].

sequence shows all the characteristics of a swarm, with the main event in the middle of the sequence and the size of the seismic cloud much larger than the rupture size of the largest event.

The population felt the 2012 and 2014 mainshocks at distances up to 250 km with an epicentral intensity of V–VI and VI (EMS-98), respectively [Sira et al., 2012, 2014]. For the 2012 mainshock, the cities located in the south felt the event more strongly than those in the north. The peak ground acceleration (PGA) value on rock-site stations was indeed eight times larger in

Nice (100 km south of the event) than in Grenoble (100 km north of the event). Courboulex et al. [2013] explain this amplitude difference by a rupture directivity southward (towards N155° E). However, no such effect was found for the 2014 event. The rupture behaviour was then different for 2012 and 2014, even though they both have similar focal mechanisms, showing a normal motion with a right-lateral strike-slip component on a fault plane oriented N155° E, 70° W (Figure 5b).

After both mainshocks, numerous aftershocks occurred. Of the 13,000 events detected by Sismalp during the period 2012–2015, ~6000 events were located and ~3000 relocated [Thouvenot et al., 2016; Figure 6a,b]. Using a 2-month temporary deployment (10/04/2014–10/06/2014) after the 2014 event, De Barros et al. [2019] detected by template matching more than 9000 aftershocks among which about ~6000 events were relocated. The 2012 cluster is about 5.5 km long, between 2 to 9 km depth while the 2014 cluster is about 11 km long, and 4 to 11 km depth [Thouvenot et al., 2016; Figure 6a,b]. The main alignment of both aftershock sequences is N155° E and is consistent with the orientation of the mainshock fault plane inferred by the focal mechanism. In detail, the spatial distribution of the aftershocks is, however, much more complex. Indeed, De Barros et al. [2019] show that the seismicity after the 2014 earthquake did not occur on the mainshock fault plane, but on several fault segments describing a thick band of seismicity. This is consistent with the fault structure observed in the Argentera Massif. Indeed, faults are likely not planar surfaces surrounded by damage zone but rather anastomosed thick bands of deformation [Baietto et al., 2009, Sanchez et al., 2010], even if the major faults (High Durance, Serenne, Bersezio, and Jausier–Tinée) are still clearly individualized. Deep earthquakes (at 7–9.5 km depth), located around the mainshock hypocentre, occurred on ~N150° E planes dipping either ~70° E or ~65° W. As those events followed Omori's law, they are thought to be triggered by Coulomb stress changes as classical aftershocks. At shallow depth (4–6 km), events aligned on N20–60° E, ~65° E or W conjugate structures that differ from the mainshock plane. Finally, some clusters of seismicity occurred outside the main cluster of events, on structures with various orientations and depths. Both the shallow families and these outside clusters
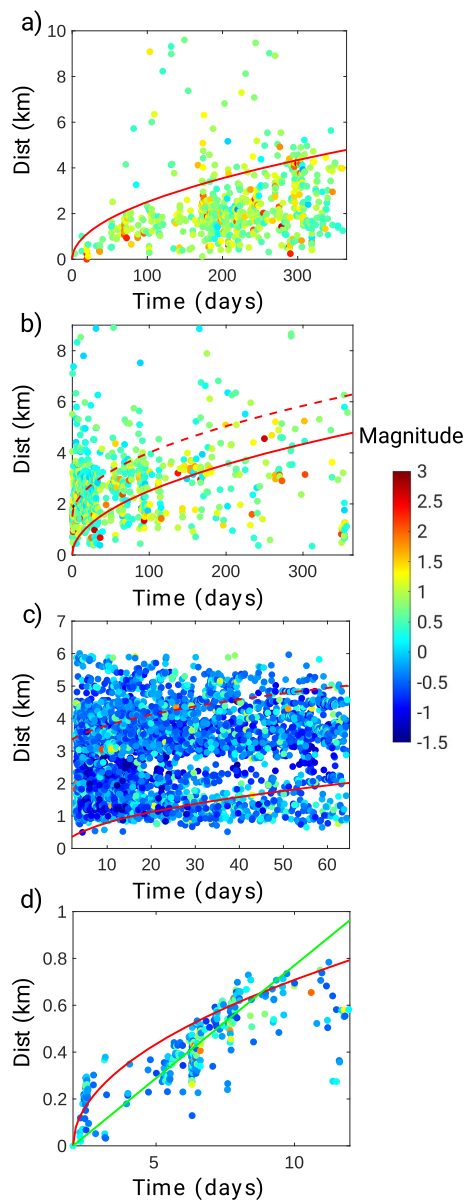
Figure 8. (**cont**.) (c) Spatio-temporal distribution after the 07/04/2014 earthquake (catalogue from De Barros et al. [2019]). For both (b) and (c), the origins are the mainshocks location and time corresponding to the purple star on Figure 6(a). Note that the first three days after the 2014 mainshock are not shown in (c) because of the incompleteness of the catalogue. (d) Spatio-temporal distribution of an isolated swarm-like family, which occurs during the 2 months following the 2014 mainshock [De Barros et al., 2019]. The origin is the first earthquake occurring in this family, and corresponds to the red square on Figure 6(a). In all panels, the colours correspond to the magnitude. The green line is the best fit for a constant velocity migration ($V = 0.1$ km/day); the plain red lines show diffusion law with a hydraulic diffusivity of $D = 0.005$ m/s^2; the red dash line is the same as the plain line, but shifted according to the rupture length of the first event [Thouvenot et al., 2016].

Figure 8. Spatio-temporal distribution of the seismicity, shown as distance–time plot. (a) Spatial–temporal distribution for the 2003–2004 swarm (catalogue from Daniel et al. [2011]). The origin point is defined as the time and location of the first event with a magnitude greater than 1, and corresponds to the green square on Figure 6(a). (b) Spatial–temporal distribution following the 26/02/2012 mainshock (catalogue from Thouvenot et al. [2016]).

do not show a clear decay of seismicity with time after the mainshock but behave as swarms inside the aftershock sequence [De Barros et al., 2019].

Thouvenot et al. [2016] show that the 2012 aftershock sequence displays a migration pattern (Figure 8b). Such migration could be fitted by a diffusion law with a hydraulic diffusivity of 0.005 m^2/s (Figure 8b), similarly to the 2003–2004 migration. On the contrary, the 2014 aftershock sequence does not show any migration (Figure 8c), as the seismicity was scattered in the full seismic cloud since the first days after the mainshock. However, within this seismic sequence, while families close to the mainshock do not show any migration, the families that occurred outside the main cluster or within its shallowest part show a diffusive behaviour (Figure 8d). Indeed, a diffusivity between 0.002 and 0.06 m^2/s, compatible with a hydraulic diffusivity, allows fitting the seismic front migration [De Barros et al., 2019; Figure 8d]. Equivalently, the migration could be fitted with a constant velocity of about 0.1 km/day [De Barros et al., 2019; green curve, Figure 8d]. This velocity seems too low to be attributed to a slow-slip event, which generally generates seismic migration

velocities of the order of 0.1 to 1 km/h [Lohman and McGuire, 2007]. Therefore, the process at play might be related to fluid-pressure diffusion. De Barros et al. [2019] proposed a conceptual model to illustrate the processes occurring at depth. Seismicity developed on conjugate fault planes belonging to the damaged zone of the main fault planes, and on some localized small faults away from the main cluster. While static Coulomb stress transfer from the mainshock might explain the seismicity occurring at depth, as classical aftershocks, fluid-driven processes were required to induce the swarm behaviour observed for the seismicity in the shallow part or outside the main cluster.

4. Discussion

4.1. *A continuous seismic activity*

Both swarms and mainshock–aftershock sequences struck the Ubaye Region with a steady activity observed since 1844. Before this date, seismicity seems to be scarcer, which is likely due to a lack of records in the historical seismicity. Therefore, a high level of seismic activity seems to be a permanent feature in this area, at least since the beginning of the 20th century. Before that, the historical data does not allow us to extend undoubtedly this observation.

According to the temporal distribution of the historical (Figure 4a) and instrumental (Figure 4b) records, the swarm occurrence seems to have a periodic pattern (Table 1). Indeed, we can notice a burst of activity, at different locations and on different faults, but every ~10 years from 1938 until nowadays (Table 1, Figures 3, 4a). Before 1938, we did not retrieve this ~10-years periodicity. This break in regularity may be associated either to a lack of events or to a lack of notice in the earthquake testimonies before 1938. Hence, even if a nearly constant periodicity can be observed for nearly one century, it is not possible to conclude if such regular activity is physically meaningful, and if so, if it is a constant or a transient phenomenon. This question is, however, of great interest, as it may help to constrain ongoing processes and bring insights for risk mitigation. In addition to a temporal regularity in the swarm occurrence, the duration of the swarms is also quite regular. Indeed, the swarms recorded by the instrumental network mainly lasted for about 1 to 2 years. The only exception is the 2012–2015 swarm, whose behaviour is intermediate between swarms and quick succession of mainshock–aftershock sequences. We cannot either generalize this observation to the historical swarms, as only a few events were noticed for each group of events. Finally, an intriguing observation is that most of the recent mainshocks (1938, 1959, 2012, and 2014) occurred in springtime. This may suggest a seasonality in the temporal distribution of the seismicity. It can be linked to the meteorological conditions, and particularly to the snowmelt periods, as observed by e.g. Deichmann et al. [2006] in the Swiss Alps. However, a deeper analysis, not yet done in any studies, should be performed to infer if such observations are of physical origin or fortuitous.

4.2. *Complex distribution of the seismicity*

The spatial distribution of the seismicity may highlight the fault traces. The 1977–1978, 1989 swarms and the background seismic activity east of Larche, St-Paul-sur-Ubaye, and Vars draw the trace of the Serenne fault (Figures 2, 5a). This alignment of seismicity is, however, very broad, as it is scattered in a 20 to 30 km large band. As event locations are determined using regional or national networks, their uncertainties might lead to an apparent scattering. Despite this methodological bias, it seems not likely that all seismic events occur on a single fault, as it would imply a fault with a very low dipping angle (<20°). Therefore, the seismicity might develop on a complex network of faults within a fractured volume. For the High Durance fault, Mathey et al. [2020] proposed a single-fault model for this structure further north. However, the distribution of the seismicity in the north part of the Ubaye Region (Figure 5a) is hardly compatible with a single-fault model as it is also widely spread. Contrary to the seismicity associated with the High Durance fault, the 2003–2004 and 2012–2015 seems to align along a single main structure, oriented N155° E that may be the prolongation to the northwest of the Jausier fault. This fault cannot, however, be seen at the surface because of the compliant sedimentary layers that cover it [e.g., Palis et al., 2016]. Therefore, we can wonder if the alignment of earthquakes is related to a single fault, to two different structures with a swarm occurring on each one, or to a complex network of smaller-length faults. At a smaller scale, the spatial distribution of the 2014 aftershocks reveals a complex network of small (hectometre to a few kilometres) structures,

both just around the mainshock fault and at kilometric distances from it [De Barros et al., 2019]. Therefore, whatever the scale, the fault network in this area appears very complex, with different orientations of structures of various lengths. It suggests a highly fractured basement inherited from the complex geological history during the Hercynian and Alpine chains formation, which probably contributes to the spatial extent of the seismicity. However, the major faults (High Durance, Serenne, Bersezio, and Jausier–Tinée) are still clearly individualized. That leads to the question, which is still opened, of the seismogenic factor of these major faults. Moreover, the presence of small faults with various orientations are indeed more likely to be reactivated as swarms, as it statically increases the chance to have faults in a near critical state. Finally, out of the Serenne and High Durance faults and the 2003–2004/2012–2015 clusters, the spatial distribution of the seismicity seems to be rather diffuse in the area. Some clusters of historical seismicity occurred close to the town of Le Lauzet, Barcelonnette, and Guillestre. However, as the detection and the precision of event locations were not optimal before 1989 and before the installation of the station SURF, it is not possible to associate those groups of events or the diffuse instrumental seismicity to any geological structures.

Most of the focal mechanisms show a dominant orientation of faults ~N150° E (Figure 5b). Such orientation is also the same as the spatial extension of relocated swarms in 2003–2004 and 2012–2015. It is also consistent with the main fault orientations in this area (Figure 2), even if most earthquakes occurred on blind, unknown faults. Using an inversion of the mechanisms based on Wallace [1951] and Bott [1959] hypothesis, the stress state was calculated for the 2003–2004 swarms [e.g., Fojtíková and Vavryčuk, 2018]. This study shows a σ1-axis N11° E, 45° ± 30°, a σ2-axis N195° E, 37° ± 30°, and a sub-horizontal σ3-axis, oriented N103° E. The stress state inferred from the 2012–2015 focal mechanism shows a similar orientation [Fojtíková and Vavryčuk, 2018].

Despite a strong seismic activity, the deformation in the area is extremely low. In the Ubaye Region, the vertical deformation determined by GPS survey is about 0.5 mm/yr and there is no measurable horizontal strain [Nocquet et al., 2016, Walpersdorf et al., 2018]. Several processes mentioned in section II (erosion, post-glacial rebound, post-slab-detachment re-

bound) may explain the low strain rate. Therefore, the seismicity might not be directly related to a large-scale deformation and to tectonic loading mechanisms. In particular, the lack of horizontal deformation seems hardly compatible with the strike-slip component without additional mechanisms.

4.3. *Processes*

As this zone shows a high seismic rate together with a low deformation rate, tectonic strain alone hardly explains the seismic profusion, and particularly, the presence of numerous swarm sequences. Additional processes are therefore likely to be involved.

The aftershocks that follow the 2012 and 2014 mainshocks may be explained by static Coulomb stress transfer from the mainshock rupture [Stein, 1999]. However, the spatio-temporal behaviours of the seismicity following the 2014 earthquake suggest that only part of the seismicity was directly triggered by stress transfer, while another process is required to explain the abnormally large number of aftershocks [De Barros et al., 2019]. In some cases, small stress or pressure perturbations are enough to trigger the seismicity that then becomes self-sustainable by stress transfer on faults that are already close to failure. Such a cascading model [Marsan and Lengline, 2008] was used, for example, to explain the high level of seismicity following the waste water disposals at low pressure in the Oklahoma state [Schoenball and Ellsworth, 2017]. Following this idea, Daniel et al. [2011] showed that about 59% of the seismic activity during the 2003–2004 swarm was triggered by stress transfer from earthquake–earthquake interaction, while the remaining part needed different processes.

An additional driving mechanism is therefore required to explain both the swarm activity and the large number of aftershocks. Either fluid pressure [Hainzl et al., 2012, Shelly et al., 2013b], aseismic slip [Lohman and McGuire, 2007, Takada and Furuya, 2010], or an interplay between both [De Barros et al., 2019, Eyre et al., 2020] are usually raised to explain swarm activity. Even if Jenatton et al. [2007] and Leclère et al. [2013] mentioned the possibility of aseismic deformation in the triggering of the 2003–2004 swarm, no evidence demonstrating the presence of aseismic slip has been found so far. The deformation is indeed too small to be seen from the

surface, and no repeating events, usually attributed to aseismic slip [e.g., Uchida, 2019] have been identified.

On the contrary, the swarm activity in the Ubaye Region is related to fluid effect in several studies on this area. The migrating seismicity in 2003–2004 [Jenatton et al., 2007], in the aftershock sequence of 2012 [Thouvenot et al., 2016] and in some clusters after the 2014 mainshock [De Barros et al., 2019] show a diffusive behaviour compatible with fluid. The velocity migration of the seismic front [$V = 0.1$ km/day, De Barros et al., 2019] is too slow to be attributed to a slow-slip event. To have such migration driven by fluids, overpressurized areas should exist in the basement. Pressure may develop in the faults, because of low-permeability structures [Sibson, 1990] or because of time-dependant creep compaction [Blanpied et al., 1992]. The faults may then act as valves [Sibson, 1990]: once the pressure reaches a failure threshold in the fault, the slip breaks the hydraulic barriers and the fault permeability is enhanced. The fluid can then diffuse, inducing migrating seismic activity along its path. Beaucé et al. [2019] also confirm the presence of fluids in the Ubaye Region, as they found that the high and continuous seismic activity shows poor temporal clustering. From the model proposed by Ben-Zion and Lyakhovsky [2006], a low temporal clustering and a high seismic activity (swarm-like) suggest fluid activity.

One of the main questions is then where the fluid is coming from and how it is trapped and pressurized at depth. The geochemical signature of geothermal springs in the Argentera massif (Figure 1) showed that water from meteoritic origin goes down to 5-to-6 km depth [Baietto et al., 2009]. As the major faults in the Ubaye Region are oriented ~N150° E and are connected to faults in the Argentera massif in the south, water from meteoritic origin may flow from this massif to underneath the Ubaye Valley [Leclère et al., 2012]. The difference of altitudes between the Argentera massif and the valley may then lead to an overpressure below the Ubaye Valley. Indeed, an overpressure equivalent to a water column of 800 m (8 MPa) or 2 km (20 MPa) is required to generate seismicity, according to Daniel et al. [2011] and Leclère et al. [2012], respectively. Such direct pressurization by meteoric fluids was also proposed to drive the seismicity in Mt. Hochstaufen [Germany, e.g., Hainzl et al., 2006] sequences. It may explain the

apparent seasonality of the seismicity, if confirmed. However, this assumption implies that losses of hydraulic heads are very limited, especially because the hydraulic path may reach about 30 km between the high summit of the Argentera and the 2012–2015 swarm.

Alternatively to this direct meteoritic pressurization, other possibilities to explain overpressure at depth require either an impervious caprock or impervious faults in their upper part. One specificity of the Ubaye area compared to the neighbouring areas is the presence of the Flysch nappes. As all the seismicity lies in the basement below these nappes, they might act as an impervious caprock. However, in this case, the seismicity is expected to be denser just beneath the nappes, which is not really observed at about 4 km depth. Alternatively, overpressurization may develop locally within the faults which show a fault-valve behaviour [Sibson, 1990]. In this case, the faults should change behaviours with time. Hydrothermal sealing processes may trap the fluid at depth which allows pressure to increase from hydrostatic to nearly lithostatic pressure [Blanpied et al., 1992, Leclère et al., 2013, 2015]. Once the pressure threshold is reached, failures (either seismic or aseismic) within the fault allow the fluid to diffuse at depth, which induces migrating seismicity.

The seismic activity, and the associated processes in the Ubaye Region, are very similar to a swarm located in Nevada (Mogul swarm), which occurred in 2008. As for the Ubaye area, this swarm took place beneath a valley with geothermal springs surrounded by high summits. The presence of fluid is necessary to explain the beginning of the swarm sequence [Jansen et al., 2019]. This seismicity may be linked to the presence of a reservoir beneath the swarm, which is filled by meteoritic water flowing from the high summit around [Ruhl et al., 2016]. From this reservoir, a fault-valve mechanism is raised to induce a migrating seismicity from the reservoir below. Same model could be applied in the Ubaye Region even if there is no evidence of a reservoir beneath the most active swarm areas. Additional measures and constraints are required to better understand the origin of the fluids and their movements at depth. For example, geophysical imagery of the fluid distribution at depth can be achieved through magnetotellurics methods or seismic velocity tomography. Geochemical analysis of a geothermal spring in the north of

Ubaye Region, such as the ones performed in the Argentera massif [Baietto et al., 2009], would also help constraining fluid flow and storage at depth.

Finally, even if fluid pressure might be considered, the alternating swarms/mainshock–aftershock sequences likely require simultaneously different processes at play. This is illustrated by De Barros et al. [2019], who showed that within the aftershock sequence of 2014, part of the seismicity was triggered by Coulomb static stress changes from the mainshock while another part showed evidence for fluid triggering. Clusters of seismicity distant from the mainshock also suggest that distant triggering through dynamic or aseismic perturbations may also occur. Such complexity in the processes, observed from aftershocks, may be spatially and temporally extrapolated to the full area. Isolated events such as background seismicity and mainshock events may be indeed attributed to tectonic stress loading, while the complex aftershock sequences and the swarms require an interplay between fluid-pressure diffusion and stress perturbations.

4.4. *Seismic hazards*

Hazards related to seismic swarms are often qualified as low, as the largest event is usually of small-to-moderate magnitude. This is the case in regions like Vogtland/West Bohemia, where regular swarms stop on their own [Fischer and Horálek, 2003, Fischer et al., 2014, Hainzl et al., 2012]. In this case, even if the regular shakings from small events bother the population locally, the seismic hazard is limited to small vibrations that have a very low probability to generate important structural damages. However, the seismic activity of swarms can also evolve towards large events, whether in continental regions [L'Aquila, e.g., Papadopoulos et al., 2010] or in subduction zones [Iquique, e.g., Ruiz et al., 2014], even if such evolution was not observed so far in the Ubaye Region. As an example, the seismic crisis (magnitudes lower than 4.0) that occurred before the L'Aquila mainshock (Mw 6.3, 2009, Italy), was first seen as a swarm of events, and led to an underestimation of the risk in this area [e.g., Papadopoulos et al., 2010]. After the mainshock (Mw 6.3) that caused about 300 casualties and extensive damages in the city of L'Aquila, this swarm was then understood as a precursory sequence. Therefore, the relationship between a seismic swarm and large earthquakes is uncertain as swarms of events can either represent the precursory phase of a large earthquake [Bachura et al., 2021, Ruiz et al., 2014] or a self-sufficient process [e.g., Hainzl et al., 2012].

Moreover, as already mentioned, the Ubaye area does not only experience seismic swarms like in 2003–2004 with a maximum magnitude smaller than 3, but also moderate size earthquakes (at least in 1935, 1938, 1959, 2012, and 2014) that generated damages to buildings [Rothé and Dechevoy, 1967, Sira et al., 2012, 2014]. The epicentral intensity often reached VI or VII (MSK-64 or EMS-98 scales, respectively). Therefore, it is important to estimate whether a larger event can occur in this area and to figure its recurring time.

The recurrence time of large events is classically extrapolated from the seismicity rate using the Gutenberg–Richter law. However, such an approach, in a context where seismicity expresses both as mainshock and swarms and where processes at play are likely complex, is definitely not straightforward. On the one hand, considering swarms as if they were a permanent contribution of the seismic rate may lead to a strong overestimation of the hazard. On the other hand, neglecting swarm activities in hazard forecasting would be spuriously safe. Therefore, estimating a recurrence time of strong, damaging events, requires first to understand and isolate the processes at play, in order to weight the contribution of swarms and mainshocks in the hazard assessment.

In the Ubaye Region, one should consider the presence of active faults due to the high rate of seismic activity, even if there is no known geological evidence of active faulting at the surface. Considering the continuity of the NW–SE trending fault system running from the Ubaye valley until the Argentera massif, a possibility would be to consider evidences of neotectonic activity reported in the latter [e.g., Ghafiri, 1995, Godel, 2003, Sanchez et al., 2010] as representative of what we cannot see in Ubaye. However, the high difference between the seismicity rates recorded in Argentera and in Ubaye then makes it difficult to easily compare the two regions. If we consider the alignment of seismicity of the 2003–2004 crisis, we can define an 8 km long structure oriented NW–SE. More or less the same

length can be obtained for the 2012–2015 sequences of aftershocks within the same direction (Figures 5c,d,e). A crude estimation of the potential magnitude can be inferred from the length of faults using classical relationship [Wells and Coppersmith, 1994]. This estimation can also be simplified by referring to Italian normal fault events that occurred in central Italy: 2009 L'Aquila Mw = 6.1 with a fault length (*L*) of 15–20 km [Chiaraluce et al., 2011]; 2016 Amatrice Mw = 6.0, *L* = 20–25 km [Bignami et al., 2019]; 2016 Norcia Mw = 6.5, *L* = 25–30 km [Improta et al., 2019]. If the full fault length highlighted by the 2003–2004 and the 2012–2015 crises was slipping at once, an earthquake of magnitude ~6 might be generated. Similarly, the complex network of the Serenne fault is long enough to generate events with magnitude larger than 6. An event of magnitude 6 or more at the same depth as the microseismicity would result in large ground acceleration and extensive damages in the epicentre region and should also be well felt in the cities of Nice and Grenoble situated 100 km away as it was for the 2012 and 2014 events. In summary, the seismic hazard of this zone should not be neglected, as the faults can potentially generate large and damaging events.

5. Conclusion

Since 1780, the Ubaye Region has been regularly affected by earthquakes, with epicentral intensities higher than VI (i.e., damaging earthquakes, MSK-64 scale). Part of this seismicity seems to occur along with the complex network of the Serenne and the High Durance faults, but also on blind structures away from these known fault systems, revealing a highly fractured medium inherited from the complex history of the Western Alps. The main fault orientation of ~N150° E is consistent with the stress state of the region, despite the very low-deforming rate measured in this area. On a larger scale, more studies are needed to make the link between the strain state in the Ubaye Region and the processes at play in the Western Alps.

This area is therefore characterized by a high rate of seismicity, that expresses either as mainshocks or as seismic swarms with low magnitude. Such complex behaviour reflects complex processes in depth that involves, in particular, overpressure and fluid diffusion. The questions of the fluid origin and how it gets overpressurized at depth remain open, despite their importance to constrain the driving processes of the seismicity. Therefore, more studies are needed to better quantify the influence of the meteoric fluid or the seasonality effect on the seismicity, and to search for the presence of possible fluid reservoirs beneath the main active areas.

Regarding hazard assessment, the main concern is the possibility that a swarm sequence could evolve towards a large mainshock or that an isolated, damaging event occurs. To address this concern, it is necessary to understand why such peculiar behaviour occurred in Ubaye Region compared to the neighbouring areas. This mainly implies not only to better understand the driving processes at the swarm scale, but also at a more regional one, as well as to better characterize the faults at depths that may carry large earthquakes.

Acknowledgements

References

Assumpção, M. (1981). The NW Scotland earthquake swarm of 1974. *Geophys. J. Int.*, 67, 577–586.

Audin, L., Avouac, J.-P., Flouzat, M., and Plantet, J.-L. (2002). Fluid-driven seismicity in a stable tectonic context: The Remiremont fault zone, Vosges, France. *Geophys. Res. Lett.*, 29, 13–21.

Bachura, M., Fischer, T., Doubravová, J., and Horálek, J. (2021). From earthquake swarm to a main shock-aftershocks: the 2018 activity in West Bohemia/Vogtland. *Geophys. J. Int.*, 224, 1835–1848.

Baietto, A., Perello, P., Cadoppi, P., and Martinotti, G. (2009). Alpine tectonic evolution and thermal water circulations of the Argentera Massif (South-Western Alps). *Swiss J. Geosci.*, 102, 223–245.

Barletta, V. R., Ferrari, C., Diolaiuti, G., Carnielli, T., Sabadini, R., and Smiraglia, C. (2006). Glacier shrinkage and modeled uplift of the Alps. *Geophys. Res. Lett.*, 33(14).

Beaucé, E., Frank, W. B., Paul, A., Campillo, M., and van der Hilst, R. D. (2019). Systematic detection of clustered seismicity beneath the Southwestern Alps. *J. Geophys. Res.: Solid Earth*, 124, 11531–11548.

Ben-Zion, Y. and Lyakhovsky, V. (2006). Analysis of aftershocks in a lithospheric model with seismogenic zone governed by damage rheology. *Geophys. J. Int.*, 165, 197–210.

Bignami, C., Valerio, E., Carminati, E., Doglioni, C., Tizzani, P., and Lanari, R. (2019). Volume unbalance on the 2016 Amatrice-Norcia (Central Italy) seismic sequence and insights on normal fault earthquake mechanism. *Sci. Rep.*, 9, 1–13.

Blanpied, M. L., Lockner, D. A., and Byerlee, J. D. (1992). An earthquake mechanism based on rapid sealing of faults. *Nature*, 358, 574–576.

Bott, M. H. P. (1959). The mechanics of oblique slip faulting. *Geol. Mag.*, 96, 109–117.

Cheloni, D., D'Agostino, N., Selvaggi, G., Avallone, A., Fornaro, G., Giuliani, R., Reale, D., Sansosti, E., and Tizzani, P. (2017). Aseismic transient during the 2010–2014 seismic swarm: evidence for longer recurrence of $M \geq 6.5$ earthquakes in the Pollino gap (Southern Italy)? *Sci. Rep.*, 7, 1–10.

Chen, X., Shearer, P. M., and Abercrombie, R. E. (2012). Spatial migration of earthquakes within seismic clusters in Southern California: Evidence for fluid diffusion. *J. Geophys. Res.: Solid Earth*, 117(B4).

Chiaraluce, L., Valoroso, L., Piccinini, D., Di Stefano, R., and De Gori, P. (2011). The anatomy of the 2009 L'Aquila normal fault system (central Italy) imaged by high resolution foreshock and aftershock locations. *J. Geophys. Res.: Solid Earth*, 116(B12).

Chiu, J.-M., Johnston, A. C., Metzger, A. G., Haar, L., and Fletcher, J. (1984). Analysis of analog and digital records of the 1982 Arkansas earthquake swarm. *Bull. Seismol. Soc. Am.*, 74, 1721–1742.

Courboulex, F., Dujardin, A., Vallee, M., Delouis, B., Sira, C., Deschamps, A., Honore, L., and Thouvenot, F. (2013). High-frequency directivity effect for an Mw 4.1 earthquake, widely felt by the population in Southeastern France. *Bull. Seismol. Soc. Am.*, 103, 3347–3353.

Courboulex, F., Larroque, C., Deschamps, A., Kohrs-Sansorny, C., Gélis, C., Got, J. L., Charreau, J., Stéphan, J. F., Béthoux, N., and Virieux, J. (2007). Seismic hazard on the French Riviera: observations, interpretations and simulations. *Geophys. J. Int.*, 170, 387–400.

Daniel, G., Prono, E., Renard, F., Thouvenot, F., Hainzl, S., Marsan, D., Helmstetter, A., Traversa, P., Got, J.-L., and Jenatton, L. (2011). Changes in effective stress during the 2003–2004 Ubaye seismic swarm, France. *J. Geophys. Res.: Solid Earth*, 116(B1).

D'Auria, L., Barrancos, J., Padilla, G. D., Pérez, N. M., Hernández, P. A., Melián, G., Padrón, E., Asensio-Ramos, M., and García-Hernández, R. (2019). The 2016 Tenerife (Canary Islands) long-period seismic swarm. *J. Geophys. Res.: Solid Earth*, 124, 8739–8752.

De Barros, L., Baques, M., Godano, M., Helmstetter, A., Deschamps, A., Larroque, C., and Courboulex, F. (2019). Fluid-induced swarms and coseismic stress transfer: A dual process highlighted in the aftershock sequence of the 7 April 2014 earthquake (Ml 4.8, Ubaye, France). *J. Geophys. Res.: Solid Earth*, 124, 3918–3932.

De Barros, L., Cappa, F., Deschamps, A., and Dublanchet, P. (2020). Imbricated aseismic slip and fluid diffusion drive a seismic swarm in the corinth Gulf, Greece. *Geophys. Res. Lett.*, 47, article no. e2020GL087142.

Deichmann, N., Baer, M., Braunmiller, J., Husen, S., Fäh, D., Giardini, D., Kästli, P., Kradolfer, U., and Wiemer, S. (2006). Earthquakes in Switzerland and surrounding regions during 2005. *Eclogae Geol. Helv.*, 99, 443–452.

Delacou, B., Sue, C., Champagnac, J.-D., and Burkhard, M. (2004). Present-day geodynamics in the bend of the western and central Alps as constrained by earthquake analysis. *Geophys. J. Int.*, 158, 753–774.

Duverger, C., Godano, M., Bernard, P., Lyon-Caen, H., and Lambotte, S. (2015). The 2003–2004 seismic swarm in the western Corinth rift: Evidence for a multiscale pore pressure diffusion process along a permeable fault system. *Geophys. Res. Lett.*, 42, 7374–7382.

Duverger, C., Lambotte, S., Bernard, P., Lyon-Caen, H., Deschamps, A., and Nercessian, A. (2018). Dynamics of microseismicity and its relationship with

the active structures in the western Corinth Rift (Greece). *Geophys. J. Int.*, 215, 196–221.

Duverger, C., Mazet-Roux, G., Bollinger, L., Guilhem Trilla, A., Vallage, A., Hernandez, B., and Cansi, Y. (2021). A decade of seismicity in metropolitan France (2010–2019): the CEA/LDG methodologies and observations. *BSGF - Earth Sci. Bull.*, 192(1), article no. 25.

Ebel, J. E. (2016). An enigmatic little earthquake swarm near searsport, Maine. *Seismol. Res. Lett.*, 87, 207–214.

Eva, E., Malusà, M. G., and Solarino, S. (2020). Seismotectonics at the transition between opposite-dipping slabs (Western Alpine Region). *Tectonics*, 39, article no. e2020TC006086.

Eva, E. and Solarino, S. (1998). Variations of stress directions in the western Alpine arc. *Geophys. J. Int.*, 135, 438–448.

Eyre, T. S., Zecevic, M., Salvage, R. O., and Eaton, D. W. (2020). A long-lived swarm of hydraulic fracturing-induced seismicity provides evidence for aseismic slip. *Bull. Seismol. Soc. Am.*, 110, 2205–2215.

Farrell, J., Husen, S., and Smith, R. B. (2009). Earthquake swarm and b-value characterization of the Yellowstone volcano-tectonic system. *J. Volcanol. Geotherm. Res.*, 188, 260–276.

Farrell, J., Smith, R. B., Taira, T., Chang, W.-L., and Puskas, C. M. (2010). Dynamics and rapid migration of the energetic 2008-2009 Yellowstone Lake earthquake swarm. *Geophys. Res. Lett.*, 37(19).

Fischer, T. and Horálek, J. (2003). Space-time distribution of earthquake swarms in the principal focal zone of the NW Bohemia/Vogtland seismoactive region: period 1985–2001. *J. Geodyn.*, 35, 125–144.

Fischer, T., Horálek, J., Hrubcová, P., Vavryčuk, V., Bräuer, K., and Kämpf, H. (2014). Intra-continental earthquake swarms in West-Bohemia and Vogtland: a review. *Tectonophysics*, 611, 1–27.

Fojtíková, L. and Vavryčuk, V. (2018). Tectonic stress regime in the 2003–2004 and 2012–2015 earthquake swarms in the Ubaye Valley, French Alps. *Pure Appl. Geophys.*, 175, 1997–2008.

Fréchet, J. and Pavoni, N. (1979). Etude de la sismicité de la zone Briançonnaise entre Pelvoux et Argentera (Alpes Occidentales) à l'aide d'un réseau de stations portables. *Eclogae Geol. Helv.*, 72, 763–779.

Fréchet, J., Thouvenot, F., Frogneux, M., Deichmann, N., and Cara, M. (2011). The M w 4.5 Vallorcine (French Alps) earthquake of 8 September 2005 and its complex aftershock sequence. *J. Seismol.*, 15, 43–58.

Fry, N. (1989). Southwestward thrusting and tectonics of the western Alps. *Geol. Soc. Lond. Spec. Publ.*, 45, 83–109.

Gardi, A., Baize, S., and Scotti, O. (2010). Present-day vertical isostatic readjustment of the Western Alps revealed by numerical modelling and geodetic and seismotectonic data. *Geol. Soc. Lond. Spec. Publ.*, 332, 115–128.

Ghafiri, A. (1995). *Paleosismicite de failles actives en contexte de sismicite moderee: application a l'evaluation de l'alea sismique dans le sud-est de la france, Paris 11.* PhD thesis.

Godano, M., Larroque, C., Bertrand, E., Courboulex, F., Deschamps, A., Salichon, J., Blaud-Guerry, C., Fourteau, L., Charléty, J., and Deshayes, P. (2013). The October–November 2010 earthquake swarm near Sampeyre (Piedmont region, Italy): a complex multicluster sequence. *Tectonophysics*, 608, 97–111.

Godel, B. (2003). Déformations actuelles dans le massif de l'Argentera-Mercantour: caractérisation des structures actives par une approche combinée géomorphologie-sismotectonique. DEA Dyn. Lithosphre Univ. Nice – Sophia Antipolis unpublished report, 114, France.

Gratier, J.-P., Ménard, G., and Arpin, R. (1989). Strain-displacement compatibility and restoration of the Chaînes Subalpines of the western Alps. *Geol. Soc. Lond. Spec. Publ.*, 45, 65–81.

Guéguen, P., Janex, G., Nomade, J., Langlais, M., Helmstetter, A., Coutant, O., Schwartz, S., and Dollet, C. (2021). Unprecedented seismic swarm in the Maurienne valley (2017–2019) observed by the SISmalp Alpine seismic network: operational monitoring and management. *C. R. Géosci.*, 353(S1), 517–534.

Guyoton, F., Fréchet, J., and Thouvenot, F. (1990). La crise sismique de Janvier 1989 en Haute-Ubaye (Alpes-de-Haute-Provence, France): étude fine de la sismicité par le nouveau réseau SISMALP. *C. R. Acad. Sci.*, 311, 985–991.

Hainzl, S., Fischer, T., Čermáková, H., Bachura, M., and Vlček, J. (2016). Aftershocks triggered by fluid intrusion: Evidence for the aftershock sequence occurred 2014 in West Bohemia/Vogtland. *J. Geo-*

phys. Res.: Solid Earth, 121, 2575–2590.

Hainzl, S., Fischer, T., and Dahm, T. (2012). Seismicity-based estimation of the driving fluid pressure in the case of swarm activity in Western Bohemia. *Geophys. J. Int.*, 191, 271–281.

Hainzl, S., Kraft, T., Wassermann, J., Igel, H., and Schmedes, E. (2006). Evidence for rainfall-triggered earthquake activity. *Geophys. Res. Lett.*, 33(19).

Handy, M. R., Schmid, S. M., Bousquet, R., Kissling, E., and Bernoulli, D. (2010). Reconciling plate-tectonic reconstructions of alpine tethys with the geological-geophysical record of spreading and subduction in the Alps. *Earth-Sci. Rev.*, 102, 121–158.

Hatch, R. L., Abercrombie, R. E., Ruhl, C. J., and Smith, K. D. (2020). Evidence of aseismic and fluid-driven processes in a small complex seismic swarm near Virginia City, Nevada. *Geophys. Res. Lett.*, 47, article no. e2019GL085477.

Hauksson, E., Ross, Z. E., and Cochran, E. (2019). Slow-growing and extended-duration seismicity swarms: Reactivating joints or foliations in the Cahuilla Valley pluton, central Peninsular ranges, Southern California. *J. Geophys. Res.: Solid Earth*, 124, 3933–3949.

Hill, D. P. (1977). A model for earthquake swarms. *J. Geophys. Res. (1896–1977)*, 82, 1347–1352.

Improta, L., Latorre, D., Margheriti, L., Nardi, A., Marchetti, A., Lombardi, A. M., Castello, B., Villani, F., Ciaccio, M. G., and Mele, F. M. (2019). Multi-segment rupture of the 2016 Amatrice-Visso-Norcia seismic sequence (central Italy) constrained by the first high-quality catalog of Early Aftershocks. *Sci. Rep.*, 9, 1–13.

Jansen, G., Ruhl, C. J., and Miller, S. A. (2019). Fluid pressure–triggered foreshock sequence of the 2008 mogul earthquake sequence: insights from stress inversion and numerical modeling. *J. Geophys. Res.: Solid Earth*, 124, 3744–3765.

Jenatton, L., Guiguet, R., Thouvenot, F., and Daix, N. (2007). The 16,000-event 2003–2004 earthquake swarm in Ubaye (French Alps). *J. Geophys. Res.: Solid Earth*, 112(B11).

Jomard, H. et al. (2021). The SISFRANCE database of historical seismicity. State of the art and perspectives. *C. R. Géosci.*, 353(S1), 257–280.

Karpin, T. L. and Thurber, C. H. (1987). The relationship between earthquake swarms and magma transport: Kilauea Volcano, Hawaii. *Pure Appl. Geophys.*, 125, 971–991.

Keranen, K. M., Weingarten, M., Abers, G. A., Bekins, B. A., and Ge, S. (2014). Sharp increase in central Oklahoma seismicity since 2008 induced by massive wastewater injection. *Science*, 345, 448–451.

Kerckhove, C. (1969). La 'zone du Flysch'dans les nappes de l'Embrunais-Ubaye (Alpes occidentales). *Géol. Alp.*, 45, 5–204.

Kerckhove, C., Cochonat, P., and Debelmas, J. (1978). Tectonique du soubassement parautochtone des nappes de l'Embrunais-Ubaye sur leur bordure occidentale, du Drac au Verdon. *Géol. Alp. Grenoble*, 54, 67–82.

Kodaira, S., Uhira, K., Tsuru, T., Sugioka, H., Suyehiro, K., and Kaneda, Y. (2002). Seismic image and its implications for an earthquake swarm at an active volcanic region off the Miyake–Jima–Kozu–Shima, Japan. *Geophys. Res. Lett.*, 29, 43–1–43–4.

Larroque, C., Baize, S., Albaric, J., Jomard, H., Trévisan, J., Godano, M., Cushing, M., Deschamps, A., Sue, C., and Delouis, B. (2021). Seismotectonics of southeast France: from the Jura mountains to Corsica. *C. R. Géosci.*, 353(S1), 105–151.

Le Goff, B., Bertil, D., Lemoine, A., and Terrier, M. (2009). Systèmes de failles de Serenne et de la Haute Durance (Hautes-Alpes): évaluation de l'aléa sismique. Rapport BRGM RP-57659-FR 84.

Leclère, H., Cappa, F., Faulkner, D., Fabbri, O., Armitage, P., and Blake, O. (2015). Development and maintenance of fluid overpressures in crustal fault zones by elastic compaction and implications for earthquake swarms. *J. Geophys. Res.: Solid Earth*, 120(6), 4450–4473.

Leclère, H., Daniel, G., Fabbri, O., Cappa, F., and Thouvenot, F. (2013). Tracking fluid pressure buildup from focal mechanisms during the 2003–2004 Ubaye seismic swarm, France. *J. Geophys. Res.: Solid Earth*, 118, 4461–4476.

Leclère, H., Fabbri, O., Daniel, G., and Cappa, F. (2012). Reactivation of a strike-slip fault by fluid overpressuring in the southwestern French-Italian Alps. *Geophys. J. Int.*, 189, 29–37.

Lohman, R. B. and McGuire, J. J. (2007). Earthquake swarms driven by aseismic creep in the Salton Trough, California. *J. Geophys. Res.: Solid Earth*, 112(B4).

Marsan, D. and Lengline, O. (2008). Extending earth-

quakes' reach through cascading. *Science*, 319, 1076–1079.

Masson, C., Mazzotti, S., Vernant, P., and Doerflinger, E. (2019). Extracting small deformation beyond individual station precision from dense Global Navigation Satellite System (GNSS) networks in France and western Europe. *Solid Earth*, 10, 1905–1920.

Mathey, M., Walpersdorf, A., Sue, C., Baize, S., and Deprez, A. (2020). Seismogenic potential of the high durance fault constrained by 20 yr of GNSS measurements in the western European Alps. *Geophys. J. Int.*, 222, 2136–2146.

Mazzotti, S., Aubagnac, C., Bollinger, L., Coca Oscanoa, K., Delouis, B., Do Paco, D., Doubre, C., Godano, M., Jomard, H., Larroque, C., Laurendeau, A., Masson, F., Sylvander, M., and Trilla, A. (2021). FMHex20: An earthquake focal mechanism database for seismotectonic analyses in metropolitan France and bordering regions. *Bull. Soc. Géol. Fr.*, 192(1), article no. 10.

McNutt, S. R. and Roman, D. C. (2015). Volcanic seismicity. In *The Encyclopedia of Volcanoes*, pages 1011–1034. Elsevier.

Nguyen, H., Vernant, P., Mazzotti, S., Khazaradze, G., and Asensio Ferreira, E. (2016). 3D GPS velocity field and its implications on the present-day postorogenic deformation of the Western Alps and Pyrenees. *Solid Earth*, 7, 1349–1363.

Nicolas, M., Bethoux, N., and Madeddu, B. (1998). Instrumental seismicity of the Western Alps: a revised catalogue. *Pure Appl. Geophys.*, 152, 707–731.

Nishikawa, T. and Ide, S. (2017). Detection of earthquake swarms at subduction zones globally: Insights into tectonic controls on swarm activity. *J. Geophys. Res.: Solid Earth*, 122, 5325–5343.

Nocquet, J.-M., Sue, C., Walpersdorf, A., Tran, T., Lenôtre, N., Vernant, P., Cushing, M., Jouanne, F., Masson, F., Baize, S., Chéry, J., and van der Beek, P. A. (2016). Present-day uplift of the western Alps. *Sci. Rep.*, 6, article no. 28404.

Palis, E., Larroque, C., Lebourg, T., Jomard, H., Flamand, A., Courboulex, F., Vidal, M., and Robert, P.-L. (2016). Earthquakes in Barcelonnette (western French Alps, 2003–2015): Where are the faults? EGU Gen. Assem. Conf. Abstr. EPSC2016-8723.

Papadopoulos, G. A., Charalampakis, M., Fokaefs, A., and Minadakis, G. (2010). Strong foreshock signal preceding the L'Aquila (Italy) earthquake (Mw 63) of 6 April 2009. *Nat. Hazards Earth Syst. Sci.*, 10, 19–24.

Parotidis, M., Rothert, E., and Shapiro, S. A. (2003). Pore-pressure diffusion: A possible triggering mechanism for the earthquake swarms 2000 in Vogtland/NW-Bohemia, central Europe. *Geophys. Res. Lett.*, 30(20).

RESIF (1995). RESIF-RLBP French Broad-band network, RESIF-RAP strong motion network and other seismic stations in metropolitan France. RESIF – Réseau Sismologique et géodésique Français. http://dx.doi.org/10.15778/resif.fr.

Ricou, L. E. and Siddans, A. W. B. (1986). Collision tectonics in the western Alps. *Geol. Soc. Lond. Spec. Publ.*, 19, 229–244.

Rothé, J. P. and Dechevoy, N. (1967). La séismicité de la France de 1951 à 1960. *Ann. IPG Strasbg.*, 3, 67–71.

Rubin, A. M., Gillard, D., and Got, J.-L. (1999). Streaks of microearthquakes along creeping faults. *Nature*, 400, 635–641.

Ruhl, C. J., Abercrombie, R. E., Smith, K. D., and Zaliapin, I. (2016). Complex spatiotemporal evolution of the 2008 Mw 4.9 Mogul earthquake swarm (Reno, Nevada): Interplay of fluid and faulting. *J. Geophys. Res.: Solid Earth*, 121, 8196–8216.

Ruiz, S., Metois, M., Fuenzalida, A., Ruiz, J., Leyton, F., Grandin, R., Vigny, C., Madariaga, R., and Campos, J. (2014). Intense foreshocks and a slow slip event preceded the 2014 Iquique Mw 8.1 earthquake. *Science*, 345, 1165–1169.

Sanchez, G., Rolland, Y., Schreiber, D., Giannerini, G., Corsini, M., and Lardeaux, J.-M. (2010). The active fault system of SW Alps. *J. Geodyn.*, 49, 296–302.

Schoenball, M. and Ellsworth, W. L. (2017). A systematic assessment of the spatiotemporal evolution of fault activation through induced seismicity in Oklahoma and southern Kansas. *J. Geophys. Res.: Solid Earth*, 122, 10–189.

Scholz, C. H. (2002). *Earthquakes and Faulting*. Cambridge University Press, Cambridge.

Scotti, O., Baumont, D., Quenet, G., and Levret, A. (2004). The French macroseismic database SISFRANCE: objectives, resultsand perspectives. *Ann. Geophys.*, 47(2), 571–581.

Segovia, M., Font, Y., Régnier, M., Charvis, P., Galve, A., Nocquet, J.-M., Jarrín, P., Hello, Y., Ruiz, M., and Pazmiño, A. (2018). Seismicity distribution near a subducting seamount in the Central Ecuadorian

subduction zone, space-time relation to a slow-slip event. *Tectonics*, 37, 2106–2123.

Serpelloni, E., Faccenna, C., Spada, G., Dong, D., and Williams, S. D. (2013). Vertical GPS ground motion rates in the Euro-Mediterranean region: New evidence of velocity gradients at different spatial scales along the Nubia–Eurasia plate boundary. *J. Geophys. Res.: Solid Earth*, 118, 6003–6024.

Serpelloni, E., Vannucci, G., Pondrelli, S., Argnani, A., Casula, G., Anzidei, M., Baldi, P., and Gasperini, P. (2007). Kinematics of the Western Africa-Eurasia plate boundary from focal mechanisms and GPS data. *Geophys. J. Int.*, 169, 1180–1200.

Shapiro, S. A., Rothert, E., Rath, V., and Rindschwentner, J. (2002). Characterization of fluid transport properties of reservoirs using induced microseismicity. *Geophysics*, 67, 212–220.

Shelly, D. R., Hill, D. P., Massin, F., Farrell, J., Smith, R. B., and Taira, T. (2013a). A fluid-driven earthquake swarm on the margin of the Yellowstone caldera. *J. Geophys. Res.: Solid Earth*, 118, 4872–4886.

Shelly, D. R., Moran, S. C., and Thelen, W. A. (2013b). Evidence for fluid-triggered slip in the 2009 Mount Rainier, Washington earthquake swarm. *Geophys. Res. Lett.*, 40, 1506–1512.

Sibson, R. H. (1990). Rupture nucleation on unfavorably oriented faults. *Bull. Seismol. Soc. Am.*, 80, 1580–1604.

Sira, C., Schlupp, A., Schaming, M., and Granet, M. (2012). Séisme de Barcelonnette du 26 Février. Rapport du BCSF 43p.

Sira, C., Schulupp, A., Schaming, M., Chesnais, C., Cornou, C., Deschamps, A., Delavaud, E., and Maufroy, E. (2014). Séisme de Barcelonnette du 7 avril 2014. Rapport du BCSF.

Špičák, A. (2000). Earthquake swarms and accompanying phenomena in intraplate regions: a review. *Studia Geophys. Geod.*, 44, 89–106.

Stampfli, G. M., Borel, G. D., Marchant, R., and Mosar, J. (2002). Western Alps geological constraints on western Tethyan reconstructions. *J. Virtual Explor.*, 8, 77–106.

Stein, R. S. (1999). The role of stress transfer in earthquake occurrence. *Nature*, 402, 605–609.

Sternai, P., Sue, C., Husson, L., Serpelloni, E., Becker, T. W., Willett, S. D., Faccenna, C., Di Giulio, A., Spada, G., and Jolivet, L. (2019). Present-day uplift of the European Alps: Evaluating mechanisms

and models of their relative contributions. *Earth-Sci. Rev.*, 190, 589–604.

Sue, C. (1998). *Dynamique actuelle et récente des Alpes occidentales internes: Approche structurale et sismologique*. PhD thesis, Grenoble 1.

Sue, C., Delacou, B., Champagnac, J.-D., Allanic, C., and Burkhard, M. (2007a). Aseismic deformation in the Alps: GPS vs. seismic strain quantification. *Terra Nova*, 19, 182–188.

Sue, C., Delacou, B., Champagnac, J.-D., Allanic, C., Tricart, P., and Burkhard, M. (2007b). Extensional neotectonics around the bend of the Western/Central Alps: an overview. *Int. J. Earth Sci.*, 96, 1101–1129.

Sue, C., Thouvenot, F., Fréchet, J., and Tricart, P. (1999). Widespread extension in the core of the western Alps revealed by earthquake analysis. *J. Geophys. Res.: Solid Earth*, 104, 25611–25622.

Sue, C. and Tricart, P. (2003). Neogene to ongoing normal faulting in the inner western Alps: a major evolution of the late alpine tectonics. *Tectonics*, 22.

Takada, Y. and Furuya, M. (2010). Aseismic slip during the 1996 earthquake swarm in and around the Onikobe geothermal area, NE Japan. *Earth Planet. Sci. Lett.*, 290, 302–310.

Thouvenot, F., Jenatton, L., Scafidi, D., Turino, C., Potin, B., and Ferretti, G. (2016). Encore ubaye: earthquake swarms, foreshocks, and aftershocks in the southern french alpsencore ubaye: earthquake swarms, foreshocks, and aftershocks in the Southern French Alps. *Bull. Seismol. Soc. Am.*, 106, 2244–2257.

Tricart, P. (1984). From passive margin to continental collision; a tectonic scenario for the Western Alps. *Amer. J. Sci.*, 284, 97–120.

Tricart, P. (2004). From extension to transpression during the final exhumation of the Pelvoux and Argentera massifs, Western Alps. *Eclogae Geol. Helv.*, 97, 429–439.

Tricart, P. and Schwartz, S. (2006). A north-south section across the Queyras Schistes lustrés (Piedmont zone, western Alps): Syn-collision refolding of a subduction wedge. *Eclogae Geol. Helv.*, 99, 429–442.

Uchida, N. (2019). Detection of repeating earthquakes and their application in characterizing slow fault slip. *Prog. Earth Planet. Sci.*, 6, article no. 40.

Utsu, T. (1961). A statistical study on the occurrence of aftershocks. *Geophys. Mag.*, 30, 521–605.

Vernant, P., Nguyen, H., Mazzotti, S., Genti, M., and Cattin, R. (2013). High uplift rates highlight the major role of erosion in the present-day geodynamics of the Western Alps. AGUFM 2013, G43A-0953.

Waldhauser, F., Ellsworth, W. L., Schaff, D. P., and Cole, A. (2004). Streaks, multiplets, and holes: High-resolution spatio-temporal behavior of Parkfield seismicity. *Geophys. Res. Lett.*, 31(18).

Wallace, R. E. (1951). Geometry of shearing stress and relation to faulting. *J. Geol.*, 59, 118–130.

Walpersdorf, A., Pinget, L., Vernant, P., Sue, C., Deprez, A., and team, R. (2018). Does long-term GPS in the Western Alps finally confirm earthquake mechanisms? *Tectonics*, 37, 3721–3737.

Wells, D. L. and Coppersmith, K. J. (1994). New empirical relationships among magnitude, rupture length, rupture width, rupture area, and surface displacement. *Bull. Seismol. Soc. Am.*, 84, 974–1002.

Yukutake, Y., Ito, H., Honda, R., Harada, M., Tanada, T., and Yoshida, A. (2011). Fluid-induced swarm earthquake sequence revealed by precisely determined hypocenters and focal mechanisms in the 2009 activity at Hakone volcano, Japan. *J. Geophys. Res.: Solid Earth*, 116(B4).